

**Here is a sample chapter  
from this book.**

**This sample chapter is copyrighted  
and made available for personal use  
only. No part of this chapter may be  
reproduced or distributed in any  
form or by any means without the  
prior written permission of Medical  
Physics Publishing.**

# Radiation Therapy

*Laurence E. Court and Lee M. Chin\**

---

11.1	Introduction and Historical Overview	288
11.1.1	Application of Radiation for Treatment of Disease	288
11.1.2	Development of Treatment Machines	288
11.1.3	Imaging Devices for Radiation Therapy	289
11.1.4	Dose Computation	289
11.2	General Issues and Processes in Radiation Oncology	289
11.2.1	Physical Basis of Radiation Therapy	290
11.2.2	Radiobiological Basis of Radiation Therapy	290
11.2.3	Detection and Staging of Tumors, and Objectives of Treatment	291
11.2.4	Treatment Planning	292
11.2.5	Patient Setup/Verification for External Beam Treatment Delivery	297
11.2.6	Dosimetry and Other QA Issues	298
11.3	Treatment Planning Processes and Tools	299
11.3.1	Treatment Simulation	299
11.3.2	Imaging Modalities Used in Treatment Planning	301
11.3.3	Dose Calculations	302
11.3.4	Treatment Planning Optimization Tools	303
11.3.5	Intensity-Modulated Radiation Therapy (IMRT) Planning	303
11.4	Treatment Delivery Processes and Tools	304
11.4.1	Description of a Medical Linear Accelerator	305
11.4.2	Localization and Verification Issues	306
11.4.3	Modern Devices	306
11.4.4	IMRT Delivery	308
11.4.5	Stereotactic Radiosurgery	309
11.5	Recent Developments and Trends	309
11.5.1	Use of Imaging Modalities in the Treatment Room	310
11.5.2	Tomotherapy	311
11.5.3	Adaptive Radiation Therapy	311

\*Corresponding author.

11.5.4	Accounting for Intrafraction Motion in Treatment Planning and Delivery	312
11.5.5	Biological Modeling	313
11.6	Conclusions	314
11.7	References	314

## 11.1 Introduction and Historical Overview

The field of radiation therapy began more than 100 years ago, with Roentgen's reporting of x-rays in 1895. This was closely followed by Becquerel's discovery of radioactivity, and then the Curies' isolation of radium from uranium ore. Soon thereafter reports began to emerge on how exposure to these new rays caused reddening of the skin, and a number of physicians realized that this was a tool that could, perhaps, cure cancer.

### 11.1.1 Application of Radiation for Treatment of Disease

The first radiation therapy successes were announced as early as 1899. Initially, the unreliability and low radiation output of the radiation production devices meant that nearly all treatments were carried out in multiple fractions. Most of treatments today are still fractionated, but now for radiobiological reasons based on extensive observations and clinical experience. Modern fractionation schemes are designed so as to kill the tumor while causing only acceptable damage to surrounding normal tissues. Instead of the 100 fractions spread over 9 months, employed in the first successful cure of a basal-cell carcinoma of the nose, treatment these days is likely to involve 30 fractions over 6 weeks.

Advances in medical physics, engineering, and radiation biology have led the evolution of modern radiation therapy. This has given rise to: treatment machines that can deliver radiation dose rapidly and with unprecedented accuracy; imaging modalities that can provide significantly improved diagnosis and localization of cancerous cells; and dosimetric instrumentation, dose calculation algorithms, and treatment planning systems that can optimize the dose distribution, so as to maximize the dose to the tumor while minimizing dose to nearby critical structures.

The importance of physics in this field is further reflected by the staffing model used by many modern cancer treatment centers, where there is approximately one medical physics staff for every two radiation oncologists.

After a brief historical review, this chapter will present an overview of the state-of-the-art of physics of radiation therapy, both clinical and theoretical; it will also suggest how the field is likely to develop over the next few years. The key elements of radiation therapy are discussed mostly in the framework of x-ray beams, although electron, proton, and

brachytherapy applications are included to distinguish their unique features.

### 11.1.2 Development of Treatment Machines

Throughout the history of radiation therapy, the introduction of new treatment regimens has often been dictated by the development of new treatment machines. One of the first breakthroughs was William Coolidge's "hot" cathode tube, developed in 1912–1913. The tube could produce peak x-ray energies of 200 to 250 kilovolts (kV), and had higher penetrating power than earlier treatment units, allowing the treatment of deeper tumors. The first treatment unit using spectra with a peak energy over 1 megavolt (MV) was carried out in 1937.

Cobalt-60, with gamma ray energies of 1.17 and 1.33 mega-electron volts (MeV), was first used as a radiation therapy source in 1951, and the first *linear accelerator (linac)* was installed in 1952. These high-energy machines allowed the treatment of even deeper tumors and, because they deposit their maximum dose some distance below the skin surface (a phenomena known as "skin sparing," described in section 11.2), physicians could now increase doses to the tumors without exposing the skin to unacceptably high levels. Linacs have evolved considerably since that time, and are now the dominant treatment modality.

Another major event was the commercialization of *multi-leaf collimators (MLCs)* in 1984. A MLC, consisting of a set of small, individually motorized collimator blades attached to the linac gantry, allowed treatment fields to be shaped to conform to the tumor without the need for heavy lead-based blocks. People soon were working on MLCs that move during treatment, with the aim of modulating the radiation intensity for better fit of dose to target. This technique, known as *intensity-modulated radiation therapy (IMRT)*, is now used in all modern radiation therapy centers, typically for at least 20% to 30% of treatments. It can shape the radiation field with an accuracy close to 1 millimeter (mm).

The evolution of *brachytherapy*, a branch of radiotherapy in which sealed radioactive materials are placed in or on the tumor, has also been led by developments in medical physics and engineering. In particular, the development of new sealed-source delivery machines and the introduction of artificially produced radionuclides. In the early days, radium was used almost exclusively. The discovery of artificial

radioactivity in 1934 eventually led to the use of many other radioactive materials for brachytherapy, including Cs-137, Ir-192, Au-198, and I-125. Because of the need to manipulate the sources, radiation exposure to staff was long a major concern. The risks have been reduced significantly, however, through the development of after-loading techniques, where empty source carriers are inserted into the patient, and the sources are introduced and removed rapidly later; the situation improved even more with the evolution from manual to remote-controlled afterloading, which virtually eliminated exposure to the staff by computer control of the insertion of the radioactive sources.

### 11.1.3 Imaging Devices for Radiation Therapy

Advances in the physics and engineering of imaging devices have had as much of an impact on radiation therapy treatments as the treatment machines themselves.

From the very start, x-ray film played a central role in the treatment planning for individual patients. The late 1960s and early 1970s saw the introduction of radiation therapy *simulators*, which are kV x-ray units with exactly the same geometry as treatment units. These allowed physicians to make “therapy-beam’s-eye-view” x-rays and fluoroscopic images with the patient in exactly the same position as for treatment, thereby revealing which organs would be irradiated. The physician could then draw the shape of the desired radiation field on the film, and beam-modifying radiopaque blocks would then be cut or molded to eliminate the beam elsewhere to shield the healthy tissues. This technique, known as *treatment simulation*, is still used today.

Computed tomography was introduced by Hounsfield in 1971, but its widespread adoption in radiation therapy was surprisingly slow, and the use of computed tomography (CT) images for radiation therapy planning did not become common until the last half dozen years. Now, in 2006, the use of traditional simulators is being phased out, and CT images form the basis for treatment planning in nearly all cases. As with traditional simulators, physicians can still see the beam’s-eye-view, and draw blocks, but now this is done using software—a process known as “virtual simulation.”

Currently, simulation (where the beam angles are decided) and treatment planning (where doses are calculated) are still kept as separate functions, but it seems likely that eventually they will combine. The clinical use of other imaging modalities, such as positron emission tomography (PET) and magnetic resonance imaging (MRI), to help define tumor volumes is also increasing, and it is likely that the trend will continue.

Imaging in the treatment room is also extremely important, and radiographic films are routinely taken (using the linac itself as the x-ray generator) to verify patient setup position. This area has recently been revolutionized, with the

introduction of *electronic portal imaging devices (EPIDs)*. A major drawback is the poor image quality resulting from the use of MV (rather than kV) x-rays.

Digital imaging allows easy electronic transfer of images, so that images can be reviewed from distant locations. It also makes possible automatic image registration techniques, which will lead to unprecedented reproducibility in patient setup. Particularly importantly, there is no film to be developed; image-guided techniques, where images are taken immediately before treatment, can therefore be employed without significant increases in patient treatment time. In-room CT imaging and other techniques are becoming commercially available, but their use has not yet spread beyond some larger research cancer centers.

### 11.1.4 Dose Computation

By the 1920s, many of the concepts underlying modern treatment planning had already been introduced, including the use of percentage depth dose curves and other information to generate isodose distributions (described in detail below). Rapid advances in electronics and computers, starting in the 1960s, led to the development of computer-based *treatment planning systems*. The complexity of early dose calculation algorithms was limited by the relatively slow computer speed, but as computers improved, so did the complexity and accuracy of the dose calculations. We now expect an accuracy of 1% to 2% for many situations, and the clinical adoption of Monte Carlo techniques, in which the path and dose deposition of each of many hypothetical photons and electrons is individually considered, is on the horizon. This will allow precise calculations for the few situations where our current techniques are less accurate, such as in the presence of a complicated and heterogeneous distribution of tissue densities.

As well as improvements in the accuracy of dose calculations, recent years have seen developments in the way radiation treatments are designed. These have provided the physician with greater ability to define the dose-distribution goals, and to optimize the radiation fields so as to best achieve this. With the exception of breast planning (which has some unique issues because of the limited number of gantry angles, and significant setup variations), virtually all IMRT plans are now developed with the aid of computer-based optimization programs, giving physicians ever greater ability to decide exactly where they want the dose to be delivered.

## 11.2 General Issues and Processes in Radiation Oncology

This section introduces some of the fundamental concepts that form the backbone of all modern radiation therapy.

These include the underlying physical and radiobiological processes, quantitative therapy planning, treatment delivery, and issues in dosimetry and quality assurance.

### 11.2.1 Physical Basis of Radiation Therapy

#### *Photon interactions in matter*

There are three main processes by which x-rays in the therapeutic energy range deposit energy in matter: the photoelectric effect, Compton scattering, and pair production. The relative interaction probability of each of these depends on the energy of the incident photon and the atomic number ( $Z$ ) of the medium (Bushburg et al. 2002; Hendee, Ibbott, and Hendee 2004; Johns and Cunningham 1983; Wolbarst 2005).

**Photoelectric effect.** In a photoelectric interaction, a photon collides with an atom, and ejects a bound electron from it. This electron has kinetic energy equal to the difference between that of the incident photon and the binding energy of the ejected electron. For soft tissue, this is the dominant interactive process for low-energy incident photons ( $<0.03$  MeV). The probability that this interaction will occur generally varies as  $Z^3$ . This is why bones (which have relatively high  $Z$ ) have high contrast in diagnostic x-ray images, and is also the cause of artifacts around high  $Z$  materials (such as tooth fillings) in CT images.

**Compton scattering.** An incident photon can scatter incoherently with an atomic electron—that is, part of its energy is expended in ejecting the Compton electron at high speed, and the rest leaves the site of the interaction as a Compton scatter photon. Compton scattering is the dominant interaction in soft tissue for incident photons between 0.1 and 5 MeV. The interaction probability is proportional to electron density, and almost independent of atomic number. This means that the presence of bone in the path of the radiation beam does not significantly alter dose to the patient downstream from the bone. It also means that x-ray images taken with high-energy x-rays do not have good contrast, and that MV CT images do not suffer from high- $Z$  artifacts. There exists another (coherent) scatter mechanism which is relevant to x-ray imaging but, since there is no deposition of energy in the exposed medium, it plays no role in therapy.

**Pair production.** This interaction occurs when a photon passes close to the nucleus of an atom, and undergoes conversion into mass, in the form of a positive and negative electron pair. It can only occur when the photon energy is above two times the energy equivalent of one electronic mass ( $2 \times 0.511 = 1.02$  MeV). Once the positron loses its kinetic energy, it interacts with an electron in the media, resulting in the annihilation of both particles, and the creation of two 0.511 MeV photons. The probability of this interaction

occurring per gram of material is approximately proportional to  $Z$ .

#### *Electron interactions in matter*

High-energy electrons may be incident on a medium from a therapeutic electron beam, or may be ejected from atoms as a result of photon interactions. As these electrons travel through the tissue, radiation detection, shielding, or other material, they gradually lose energy until they are slow enough to be captured by atoms. The main processes by which electrons lose energy are through Coulombic (electric) interactions with either atomic electrons or atomic nuclei:

**Inelastic electron collisions with atomic electrons.** The rate of energy loss through the excitation or ionization of atomic electron clouds depends on the electron density, and tends to be lower for higher- $Z$  materials, whose electrons tend to be more tightly bound. For high-energy electrons, with energies above 1 MeV, the rate of energy loss in passage through water or soft tissue is fairly constant at 2 MeV/cm. This is important, as it determines the maximum depth to which electrons will penetrate; e.g., if a 9-MeV electron beam is used to irradiate a neck node, the spinal cord will receive a very low dose if it is 4.5 cm or more deep.

**Inelastic collisions with atomic nuclei.** Bremsstrahlung x-ray energy loss occurs when an electron passes near a nucleus and is deflected and accelerated by its Coulombic field. The probability of occurrence of a bremsstrahlung interaction increases with electron kinetic energy and with  $Z$ . This interaction is of particular importance in the targets of both diagnostic x-ray tubes and linacs, where high-energy electrons interact to produce high-energy photon beams.

High-energy photo- and Compton electrons follow tortuous paths through tissue because of multiple Coulomb scatterings. The scattering cross-section is approximately proportional to  $Z^2$  and inversely proportional to the electron energy. (High-energy *protons* from an accelerator, by contrast, interact with matter in a similar fashion, but the protons scatter significantly less, and leave behind a nearly straight trail of ionizations.)

### 11.2.2 Radiobiological Basis of Radiation Therapy

Radiation therapy involves the killing of all cancer cells and the sparing of enough healthy cells.

Radiation may interact with biologically important molecules in tissue, in particular DNA (direct action), or with water, which, upon its excitation or ionization, transforms into highly reactive chemical species (free radicals) that themselves damage biological molecules (indirect action). About two-thirds of the biological damage by x-rays is due to indirect action, which can be modified by chemical sensitiz-

ers or protectors. The sensitivity of cells to irradiation is determined by four biological processes (known as the four Rs) (Hall 2000):

### Repair

There are four main types of radiation-induced DNA lesions: DNA protein crosslink, base alterations, single-strand breaks, and double-strand breaks. Three of these are either infrequent (DNA protein crosslinks) or efficiently repaired (base alterations and single-strand breaks). Double-strand breaks are less frequent than base alterations and single-strand breaks but are repaired very inefficiently, meaning that this is the most important form of cellular damage. (All four mechanisms are capable of playing a role in the separate but related process of radiation carcinogenesis.) Radiation therapy tends to be more effective in situations where normal tissue can undergo repair faster than tumors.

### Repopulation

Given time, some types of undamaged cells will divide and repopulate, replacing those that were killed by the irradiation. Ideally, this will occur more rapidly in healthy tissues, as with repair.

### Redistribution

Different phases of the cells cycle are more resistant to radiation than others. After irradiation, more cells are left in radiation-resistant phases than in sensitive phases, meaning that an immediate subsequent irradiation would be less successful in killing tumor cells. Ideally, treatments would be timed so that the cohort tumor cells had returned to a sensitive phase, while the healthy cells had not.

### Reoxygenation

Hypoxic (oxygen-starved) cells are particularly resistant to radiation damage. Because of the limited diffusion distance of oxygen in tissues, cells at the center of a pocket of tumor may be hypoxic, and therefore more difficult to kill, than those surrounding it. By spreading the irradiation over many fractions, so that outer portions of the tumor are killed, previously hypoxic regions may become oxygenated, and therefore more sensitive to irradiation.

The relative importance and effectiveness of these processes can be significantly different for different tissues. For example, rapidly dividing cells, such as cells of skin or the lining of the gut, are more sensitive to irradiation than nondividing cells, such as neurons. The radiation sensitivity of cells can be described with cell survival curves, such as in Figure 11–1, where one curve applies to late-responding tissues (e.g., lung or kidney), and another to a tumor or early-responding tissue. At low doses, the late-reacting normal tissues appear to be better at repairing themselves. This is

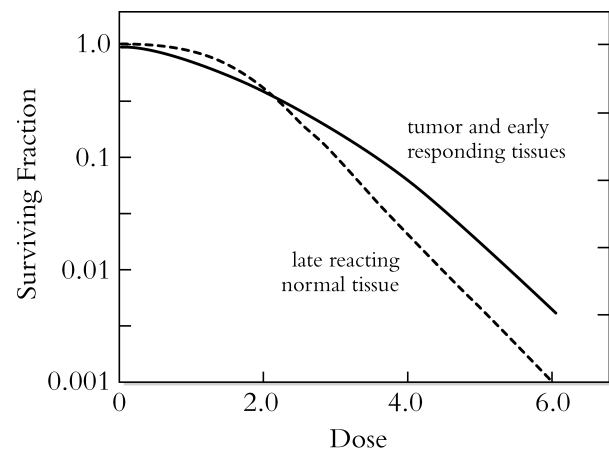


**Figure 11–1.** Cell survival curves relating surviving fraction to dose for late reacting tissues and tumors/early-responding tissues.

another biological reason for fractionation. The shapes of these curves mean that by splitting the delivery of a large prescription dose into multiple smaller fractions we can achieve significantly better survival of normal tissues but still slowly kill the tumor cells.

### 11.2.3 Detection and Staging of Tumors, and Objectives of Treatment

#### Cancer detection

Cancer may be found when a symptomatic patient visits the physician. Alternatively, it may show up as part of a regular cancer-screening program, one designed to detect disease in its early stages, even before symptoms appear. Some common tests (DeVita, Hellman, and Rosenberg 1997; Perez and Brady 1987) are:

- *Breast cancer screening.* This is carried out through a combination of breast self-examination, clinical breast examination by a trained professional, and mammography (x-ray imaging of the breast). Breast cancer screening, recommended by the National Institutes of Health (NIH), American College of Radiology (ACR), and other leading organizations for women aged 50 years and over, can be life saving.
- *Colorectal cancer screening.* If colorectal cancer can be detected and treated while it is still in its early stages, and is still localized, then 5-year survival rates of 85% or higher can be achieved. This drops to 50% to 60% once the cancer has spread, thus emphasizing the importance of screening. Screening tests include digital rectal examination, stool blood test, sigmoidoscopy (a flexible endoscopic tube is inserted into the rectum, and images are taken of the rectum and colon), and, recently, CT-base “virtual” colonoscopy.
- *Prostate cancer screening.* As with other cancers, detection of prostate cancer at its earliest stages has a

significant impact on 5-year survival rates. Screening tests include digital rectal examination and testing for elevated levels of prostate-specific antigens.

- *Cervical cancer screening*—by means of the Pap smear test and clinical pelvic examination.

### Cancer staging

Once a cancer has been detected, it is important to establish its *stage*; that is, how much it has already grown and/or spread. Staging is a primary factor determining the optimal therapy modality (surgery, radiation therapy, chemo or hormonal therapy, etc.) or combination of modalities. It also is important in planning the patient's treatment, facilitates information exchange between all the professional staff involved in the treatment, and allows for an estimate of the probability of success of the therapy. A common method of staging is the TNM system, which is based on the size of the tumor (T0 to T4), the extent to which it has spread to the lymph nodes (N0 – N3), and the presence or absence of distant metastases (M0 and M1).

### Treatment goals

The objectives of therapy depend on the type, location, and staging of the cancer. The goal may be to bring about a complete cure by destroying all the cancer cells, thereby extending the patient's disease-free life. For many patients cure is not possible, unfortunately, but it may still be possible to palliate some of the symptoms (e.g., obstruction of the bowel or airway) by reducing the tumor mass.

### Therapeutic ratio

The therapeutic ratio describes the susceptibility of the tumor to radiation damage, relative to the sensitivities of the nearby normal tissues. Increasing the dose improves local tumor control (i.e., probability of killing all tumor cells), but this also increases the likelihood of damaging normal tissues (Figure 11–2). It is possible to manipulate the treatment to maximize the therapeutic ratio, thus increasing the probability of local control (i.e., prevention of local recurrence) without inducing serious complications. Some ways of doing this include irradiating the tumor with beams coming in from multiple angles, and catching it in their cross-fire region; selecting the beam angles so as to avoid sensitive structures; conforming the treatment beams to the shape of the tumor using lead blocks or collimators, thus avoiding noncancerous tissues; and treating superficial tumors with electron beams (which have relatively low penetration power, and therefore avoid irradiation of deeper structures).

#### 11.2.4 Treatment Planning

Conventional radiation therapy treatments are planned in three steps. First, the radiation oncologist must determine the

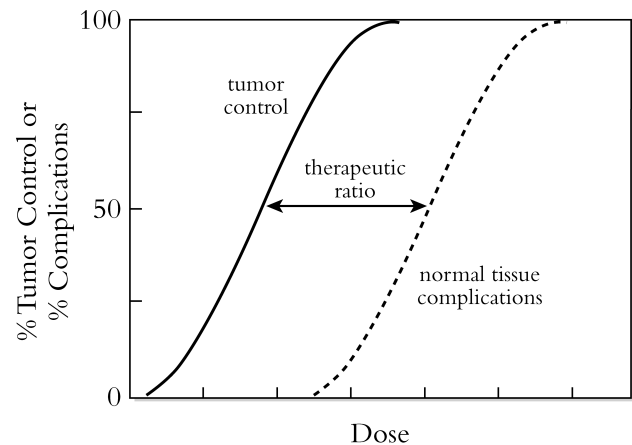


**Figure 11–2.** The relationship between tumor control, complications, dose, and therapeutic ratio in radiation therapy treatment planning.

location and extent of the volume to be treated, and also of any critical structures that must be spared. The staff then have to decide on the treatment modality (which depends on the tumor location and the characteristics of the available beams), on the number and angular distribution of the beams, and on the need for any beam modifiers to change the shape or intensity distribution of the radiation field (Kahn 1994; Bentel 1996). After this is all done, the dosimetrist calculates the dose distribution in tissue in the treatment-planning computer, and displays it for inspection. Several iterations may be required in the second and third steps before an acceptable plan is obtained.

### Planning volumes

One of the aims of radiation therapy is often to conform the dose to a specific volume, thus avoiding unnecessary, and potentially harmful, dose to normal tissues. Several definitions help remove any potential ambiguity in how volumes are determined (ICRU 1999; Prado and Prado 2004). The *gross tumor volume (GTV)* is the volume of known disease, such as disease visible on a CT image (Figure 11–3). The *clinical target volume (CTV)* is the GTV, but expanded to include regions of suspected subclinical, microscopic malignant disease that may not be visible or palpable; the CTV must be treated if local failure is to be avoided. The *planning target volume (PTV)* is a geometric expansion in three-dimensions (3-D) that accounts for geometric uncertainties that can arise from daily variations in patient setup and intra- and interfraction motion of the target volume (caused, for example, by breathing). Finally, the *treated volume* is the four-dimensional (4-D) volume (3-D + motion/time) of tissue to which the prescription dose is actually delivered.

These volumes are usually identified on a CT image of the patient, although other imaging modalities can be used (see section 11.3.2). The specifics of how they are established depend on the clinical site. In radiation therapy of the

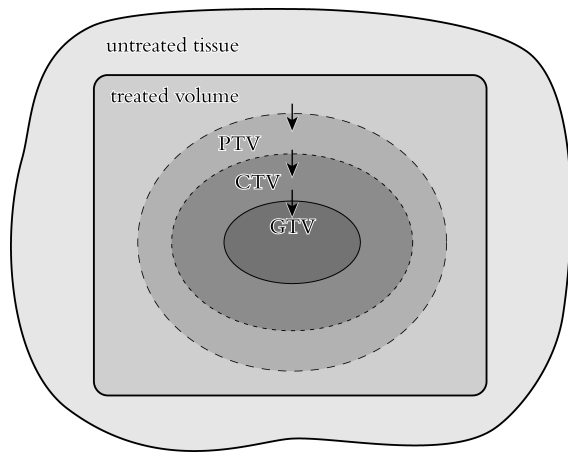


**Figure 11-3.** Definitions of volumes used in radiation therapy: gross tumor volume (GTV), clinical target volume (CTV), planning target volume (PTV), and treated volume.

prostate, for example, the GTV is the prostate itself, as seen in CT or MRI images; the CTV also is the prostate, if there is no subclinical spread of disease outside the prostate. Because the position of the prostate can change significantly from day to day, the PTV is typically expanded by 0.5 to 1 cm in all directions. This PTV expansion can increase the treatment volume by a factor of 3 to 4, which is why one of the aims of modern radiation therapy is to develop ways of reducing the setup uncertainties, thus decreasing the necessary PTV expansion.

#### Characteristics of therapeutic external beams

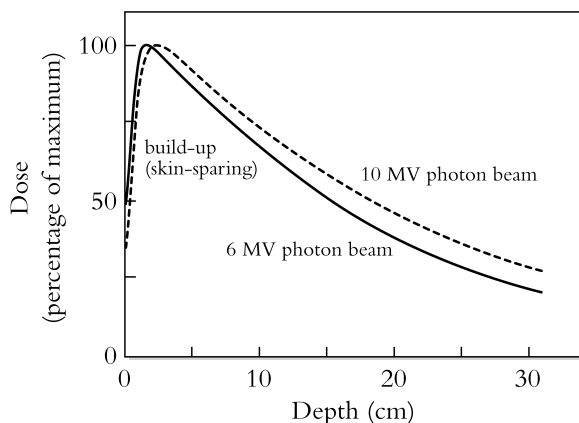
The variation of deposited dose with depth along the central axis of a beam is described by way of *percentage depth dose* (PDD) curves (Figure 11-4a).

**Photon beams.** The shape of the PDD curve for high-energy photons can be explained in the following way: Photon interactions in the patient's surface tissues result in the ejection of high-energy electrons which deposit their energy some distance downstream. At progressively greater depths, more and more electrons become involved. This gives an initial increase in dose in the build-up region, until a maximum is reached at a depth,  $d_{\max}$ , characteristic of the beam energy. This gradual dose build-up near the surface accounts for the *skin-sparing effect* (the skin, which is relatively sensitive, is "spared" because it receives less dose than slightly deeper tissues). Because the photon fluence is decreasing with depth due to both attenuation and (usually to a lesser extent)  $1/r^2$  falloff, the density of high-velocity free electrons falls off with depth, hence a *falloff* in dose with depth beyond  $d_{\max}$ , as indicated by the PDD.

The dose distribution can be displayed as *isodose curves*, which are lines connecting the points that receive the same particular dose (Figure 11-4b). The dose tends to be nearly uniform across the central region of a broad beam; the shape of the dose distribution at the edges of and outside the beam, however, depends on the geometric penumbra (resulting from the finite size of the linac's focal spot), collimation, and beam energy (i.e., to what extent photons are scattered in the forward direction).

**Electron beams.** Electron beams can also be characterized with PDD curves and isodose distributions. The electron beams of Figure 11-5a also have a skin-sparing effect, although this is less pronounced than with photon beams; it is determined by the effective increase in fluence that results from electron scattering and ionization in the media. After the build-up region there is a reasonably flat region of

a



b

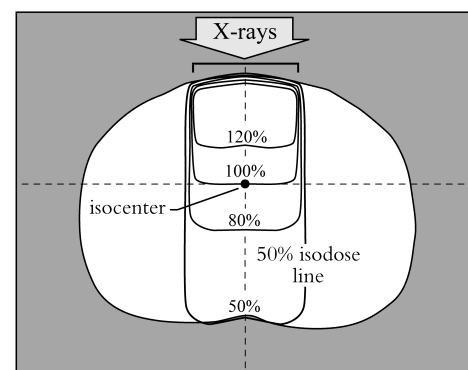


**Figure 11-4.** Percentage depth dose and isodose curves for photon beams. (a) PDD curves for 6 MV and 10 MV photon beams; (b) isodose distribution for a single incident 6-MV beam.

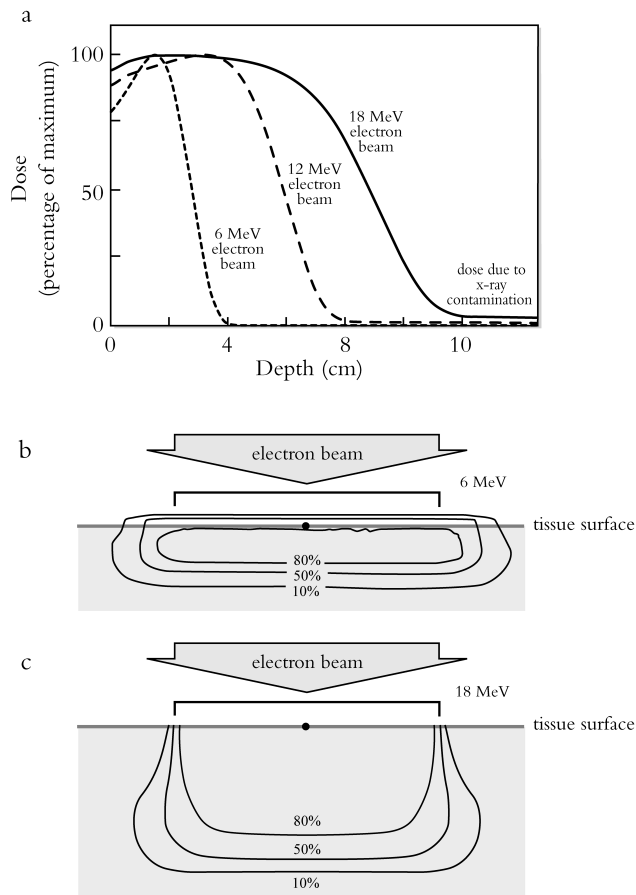


**Figure 11-5.** Percentage depth dose curves and dose distributions for electron treatment beams. (a) PDDs for electron beams of several energies; (b) dose distributions for a low-energy (6 MeV) electron field; and (c) for a high-energy (18 MeV) electron field.

high dose, followed by a rapid falloff. Electrons lose energy at about 2 MeV per cm of water or soft tissue so that, as noted earlier, there is virtually no dose deposited by the electrons beyond their maximum range (although there is a small residual dose due to x-rays produced by bremsstrahlung interactions in the linac head). This sharp falloff is one of the primary advantages of electron beams, as it allows sparing of critical structures that are slightly deeper than the target volumes. The shape of isodose curves for electron beams is determined by how the electrons are scattered in the patient. For beams of a few MeV, all isodose levels bend out below the skin surface. For high-energy beams, only the low isodose levels bow out. This bowing can make the placement of several adjacent electron fields difficult, and result in regions of high or low doses (known as hot or cold spots).

**Proton beams.** Both x-ray and electron PDDs are characterized by a build-up region, followed by a decrease in absorbed dose with increasing depth. Proton beam PDDs are very dif-

ferent, being fairly constant until they have penetrated to their greatest depth, where a sudden and large peak occurs (Figure 11-6). As with electrons, and unlike x-rays, there is no dose beyond the practical range—the protons gradually lose kinetic energy as they pass through and ionize the medium. Towards the end of their range, where they have little energy left and are traveling very slowly, they experience a large increase in stopping power, giving a peak (known as the *Bragg peak*) in absorbed dose. The depth at which the Bragg peak appears can be controlled by altering the energy of the incident protons. Careful selection of the proton energy can be used to direct the absorbed dose onto a deep tumor, while maintaining low doses to normal tissues at shallower depths, and virtually zero dose to deeper tissues. The same thing happens also with electron beams, but the multiple scattering they experience as they slow down smears out their Bragg peak completely.

#### Arrangements of external beams

There are several typical arrangements of beams used to deliver dose to the target volumes.

**Single field.** A single-photon field gives a nonuniform dose distribution, with maximum dose 1.5 to 3.5 cm below the skin surface, depending on the x-ray energy. It is appropriate for treating some relatively superficial sites, such as the supraclavicular lymph nodes. The relatively high subcutaneous dose means that single fields are usually not suitable for deeper target volumes.

The limited range of an electron beam means that it is normally used only as single field for superficial tumors—for example as a boost in treatment of the breast.

#### Opposed fields

Parallel-opposed fields deposit their dose uniformly (Figure 11-7a). This is a simple and effective way of distributing dose uniformly over a target volume, and it is quick and easy

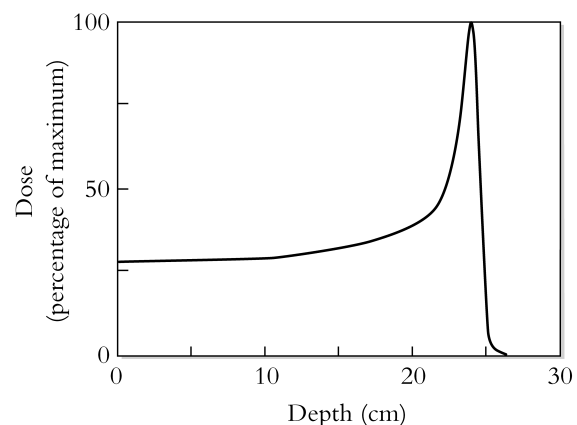


**Figure 11-6.** Percentage depth dose for a proton beam.

to reproduce daily for treatment. Opposed fields have high-dose regions in the subcutaneous tissues, and the magnitude of this effect depends on the beam energy, patient thickness, and field size.

If the tumor is centrally located, and if it is necessary to minimize dose to surrounding tissues, then it is useful to increase the number of treatment beams.

**Four-field box.** The four-field box technique (Figure 11–7b) consists of two pairs of opposed beams, crossing each other orthogonally in the center of the target. The high-dose region is rectangular (hence the name “box”), and is fairly homogeneous. A particular advantage of doubling the number of radiation beams is that the subcutaneous dose is now distributed over four areas, rather than two.

These are the simplest beam arrangements—there are many more complicated arrangements, with more beams, different incident angles (including rotational beams), for dealing with more complex geometries.

**Beam modifiers for photon irradiation.** A linac produces a fairly flat, rectangular radiation field. Such a field could result in some undesirable irradiation of normal tissues, so it is

often necessary to modify the beam shape or intensity distribution. This can be achieved with:

- *Shape modifiers.* The shape of the treatment field can be customized using cerrobend™ (a lead alloy) blocks. These are individually molded, based on a beam’s-eye-view of the PTV, typically with a margin of around 7 mm to account for beam penumbra. This technique of conforming the shape of the radiation field to the target (rather than using simple open rectangular fields) is known as *conformal therapy*. A modern linac can shape the radiation field with a MLC, which consists of many individually motorized, thin-slice sheets of collimator material (see section 11.4.3).
- *Intensity modifiers.* The most common method of modifying the intensity is by way of wedge-shaped metal attenuators, which are inserted in the beam to give tilted isodose curves (Figure 11–8) or to compensate for sloping skin surfaces. Modern linacs achieve the same effect by actively moving one of the collimators across the field while the beam is on—a process known as dynamic, or virtual, wedging. As well as removing the need for handling heavy accessories, *dynamic wedging* has the additional advantage doing away with the position-dependent beam-hardening (where the x-ray spectrum is changed by preferential attenuation of low-energy x-rays) caused by the continuously varying thickness of attenuating material in a standard wedge, which can make dose calculations more complex. Even more complex intensity modulation can be achieved by moving the leaves of MLCs across the radiation field while the beam is on. This process, called intensity-modulated radiation therapy (IMRT), is discussed in detail later (see section 11.3.5).
- *Bolus.* This is a piece of flexible, tissue-equivalent material that is placed directly on the skin. Unlike wedges located distant from the skin, here the effect is to move the depth of maximum dose closer to the skin surface. Bolus is used when high-energy x-ray beams are being used to simultaneously treat deep and superficial targets (such as scar tissue). Without the bolus, the skin-sparing effect would result in underdosing of the target.

**Beam modifiers for electron irradiation.** Electron beams produced by linacs are also fairly flat and symmetrical. As with photon beams, it is possible to modify the distribution:

- *Shape modifiers.* As with a photon beam, the shape of electron beams can be modified with lead cutouts. Because electrons scatter much more than photons,

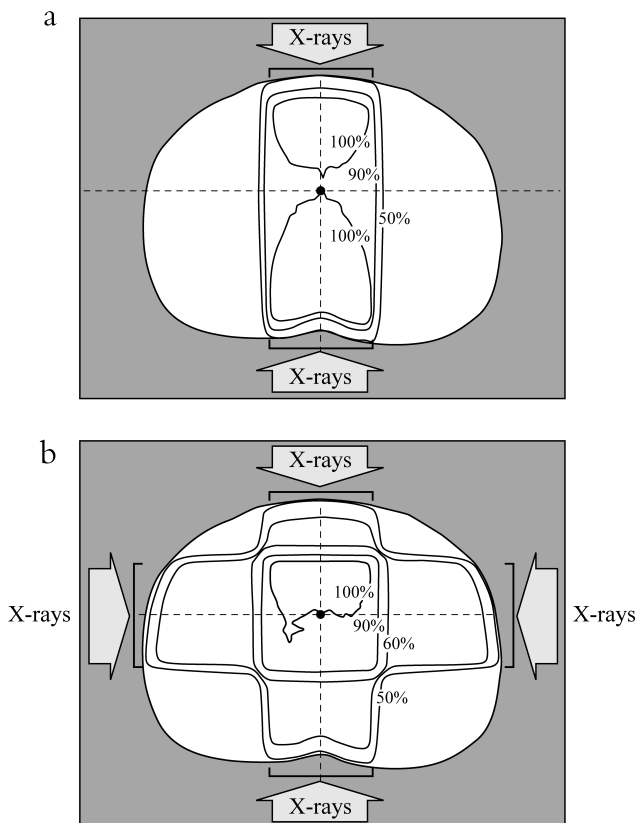


**Figure 11–7.** Dose distributions for standard plans. (a) Opposed two-field arrangement, and (b) four-field box plan.

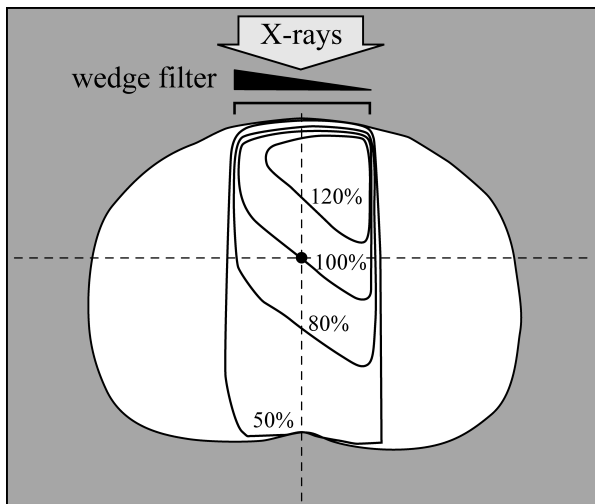


**Figure 11-8.** Effect of a wedge on a dose distribution.

these cutouts must be placed either on the patient's skin, or at the end of the electron treatment cone, close to the skin. Situating them closer to the linac head, as is done with photon beams, would result in a large penumbral region. Currently there are no commercial MLCs suitable for electron treatments.

- **Bolus.** Bolus, when used with electron beams, increases surface dose and reduces the depth of maximum penetration. This is useful to increase the dose to the skin, or when there is a relatively shallow critical organ in part of the field. Bolus can also be used to flatten irregular surfaces.

### Brachytherapy

Brachytherapy refers to the placement of sealed radioactive sources in or on the tumor directly, giving a very localized dose while (because of the inverse square effect) sparing more distant normal tissues. Typical falloffs of radial doses are dominated by the  $1/r^2$  effect.

Brachytherapy can be used alone, or in combination with external beam radiation therapy. The radiobiological basis of brachytherapy is the same as that for external radia-

tion therapy, but of the 4Rs (repair, repopulation, redistribution and re-oxygenation), repair and repopulation are most important. Re-oxygenation may influence low-dose-rate permanent implants (e.g., I-125 implants for prostate cancer) to some extent, and redistribution has no impact.

**Characteristics of radioactive sources used in brachytherapy.** Brachytherapy sources are characterized by their half-life, radiation energy, and physical form (typically seed or wire) (Table 11-1), and strength (exposure rate). Radium-226, the original brachytherapy source, is no longer used because of radiation safety concerns.

**Brachytherapy application techniques.** There are several standard ways in which brachytherapy sources can be used to treat tumors; the choice depends on the size and location of the tumor.

- **Interstitial brachytherapy.** This refers to the insertion of radioactive sources directly into the tissue. The sources may be permanently implanted, such as when I-125 seeds are placed in the prostate, or may be removed after the required dose has been delivered ("temporary implants"). The advantage of a permanent implant is that it involves a one-time procedure. A temporary implant, on the other hand, allows better control (and, correction, if need be) of the source distribution and resultant dose distribution.

With a typical temporary implant, one or several catheters are first inserted into the tissues. Dummy sources are then inserted into the catheters, and x-ray images (usually planar, but sometimes CT) are taken and used to localize the sources and calculate the dosimetry. After that, the real radioactive sources are inserted, and removed after the required dose has been delivered. In cases where the dose-rate from the sources is very high, the sources are inserted remotely, using a computerized afterloading system.

- **Intracavitary brachytherapy.** The insertion of radioactive sources into a cavity in the body is used most often for treating uterine cancers. Recent innovations

**Table 11-1.** Physical characteristics of some radionuclides employed in brachytherapy.

Isotope	Half-life	Energy of emitted photons (MeV)	Encapsulated form	Permanent/Temporary
Ir-192	74 days	0.136–1.06	Seeds or wire	T
Pd-103	17 days	0.0201,0.023	Seeds	P
I-125	60 days	0.0355	Seeds	T, P
Cs-137	30 years	0.662	Pellets or tubes	T
Au-198	3 days	0.412	Seeds	P

make it possible to place them directly into the cavity created by a lumpectomy procedure for breast cancer. Intracavitary brachytherapy is always temporary, and, as with interstitial brachytherapy, the radioactive sources are handled either manually or remotely, depending on the strength of the sources.

- *External applicators.* When the tumor is close to the skin surface, molds can be made to conform to the patient's surface, and the radioactive sources inserted into tubes 0.5 to 1.0 cm away from the skin surface. This may be preferable over external beam techniques for complicated irregular external surfaces.

**Dose-rates in brachytherapy.** Unlike external beam radiation therapy, where almost all treatments are delivered at dose-rates between 200 and 1000 cGy/min, brachytherapy treatments fall into two different camps: Low dose-rate (LDR) brachytherapy and high dose-rate (HDR) brachytherapy.

**Low dose-rate brachytherapy.** LDR is delivered using dose rates of 10 to 100 cGy/hr. Because LDR has been around since the beginning of the twentieth century, there is a wealth of data both on patient survival rates and on early and late tissue complications rates, and it is well understood. The long treatment times (can be several days), however, can have important disadvantages. In particular, the extended treatment time means that there is more chance of applicator movement (which may affect the dosimetry). Also, hospitalization is necessary, and additional precautions to prevent radiation exposure to medical staff are needed.

**High dose-rate brachytherapy.** HDR uses significantly higher dose rates ( $>10^3$  cGy/h). The potential late toxicity caused by large doses per fraction is controlled by careful fractionation schemes. Most clinics are moving towards HDR, reducing their use of LDR (except for permanent prostate implants).

#### *Display of calculated doses for external-beam treatment and brachytherapy*

Various algorithms (described in section 11.3) have been designed for calculating the distribution of dose deposited in tissues from a given set of beams or brachytherapy sources. The final dose distribution is displayed as a set of isodose curves, usually superimposed on a CT image of the patient.

The distribution of doses within the patient may thereafter be presented in the more compact form of a *dose-volume histogram (DVH)*. The DVH is a plot of the volume versus the minimum dose given to that volume. For the example of Figure 11-9, 100% of the PTV gets 50 Gy, 50% gets 60 Gy, and none gets more than 65 Gy. The DVH for a PTV is characterized by a high percentage of the volume getting the pre-

scription dose, followed by a rapid falloff above this dose. The DVH for an organ-at-risk tends to have a more gradual falloff. The DVH is used to evaluate the treatment plan, taking account of published data on normal tissue tolerance doses. Normal tissue tolerance doses are typically expressed as the probability of 5% complication within 5 years from treatment (TD 5/5) and the probability of 50% complication within 5 years from treatment (TD 50/5). The TDs 5/5 for partial irradiation of the liver, for example, are 5 Gy, 3.5 Gy, and 3 Gy for exposure of 1/3, 2/3, and 3/3 of the liver, respectively. The exact tolerance doses are different for each patient (although we do not know patient-specific values), and are also a function of the treatment technique (e.g., daily dose).

#### 11.2.5 Patient Setup/Verification for External Beam Treatment Delivery

There are three essential steps involved in treatment delivery: patient positioning, the beam-on treatment itself (discussed earlier), and documentation ("record-and-verify").

##### *Patient positioning*

The important concepts in patient setup are immobilization, localization, and verification.

**Immobilization.** Because we treat the patient using the same treatment fields daily, it is important that he or she be in the same position every day, and not move during treatment. Various immobilization devices are used to satisfy both of these needs, including:

- *Alpha cradles.* These are Styrofoam™ forms that approximately match the shape of the patient's body for which they are used. The shape of the cradle is

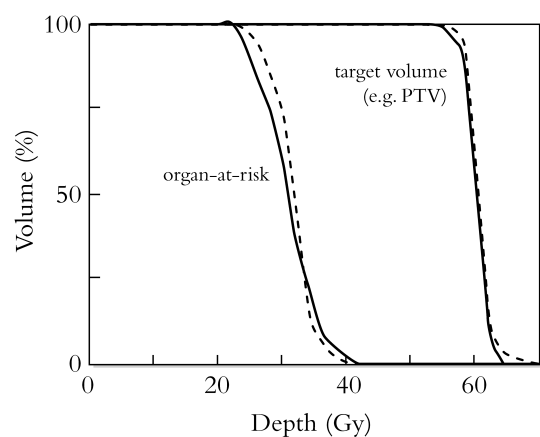


**Figure 11-9.** Dose-volume histograms (DVHs) for an organ-at-risk and for the target volume, obtained from two competing radiation therapy plans (solid vs. dotted). They are different but similar, with the dotted-line plan giving better coverage of the target, but higher dose to the organ-at-risk. It is difficult to say, on the basis of these DVHs, which plan is clinically better, or even if either is adequate.

customized using a foam-forming mixture to create a solid mold.

- *Vacuum bags.* These bags contain small polystyrene balls. When the bag is semi-deflated, it can be shaped to the patient's body. The air is then pumped out, and the bag is transformed into a solid mold.
- *Thermoplastics.* These materials become soft and pliable when soaked in warm water, and can then be stretched over the patient. When the thermoplastic cools, it regains its rigidity, providing a mold. These types of immobilization device are used particularly often when treating tumors in the head and neck region.

**Localization.** This is the process of aligning points in the patient with the same points in the treatment plan. The common point in the different systems is the isocenter, at the intersection of the axes of rotation of the linac gantry, the linac collimator, and the patient couch (Figure 11–10). Typically the patient is set up by aligning skin marks (tattoos) with laser lines that come in from both sides and from above. These lines are parallel to the patient axis, and intersect at the isocenter. Depending on the immobilization device used, localization may be possible by aligning the lasers with marks on the immobilization device itself, thus avoiding the variability associated with skin marks.

**Verification.** Localization is typically carried out using external (skin) marks, but the tumor may be deep within the body. Verifying the correctness of the patient setup typically involves taking orthogonal x-ray films, where the linac is used as the x-ray source. Because these images are taken with high-energy photons (typically 6 MV), they differ from diagnostic images in two ways. First, they display low contrast; portal images do not achieve the high contrast provided

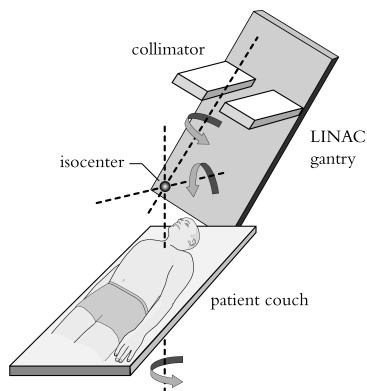


**Figure 11–10.** Location of the treatment isocenter, at the intersection of the axes of rotation of the patient couch, linac gantry, and collimator system.

by the photoelectric interactions that occur at lower energies. Second, and of less significance, the doses are relatively high, on the order of 2 to 10 cGy; special film cassettes are employed, but these still have poor quantum efficiency for high-photon energies. The dose is only a small fraction of the therapeutic dose, which is typically 180 to 200 cGy/fraction, but it has to be included when calculating total dose.

### *Record and verify (R&V)*

A critically important function of data management in radiation treatment centers is to prevent treatment errors. Radiation treatments in modern centers are managed and monitored using special record and verify software, which tracks the treatment parameters—if a patient is to be treated with electrons and a gantry angle of 30°, for example, the R&V software will not let the linac beam be turned on if it is set to photons, say, or to a different angle. The user may be able to override these interlocks if necessary, but the software effectively prevents accidental mistakes. Such software is absolutely essential for advanced techniques such as IMRT, as will be seen later.

### 11.2.6 Dosimetry and Other QA Issues

The disagreement between calculated dose at a point in the patient and the dose actually delivered should be less than 5%. Differences between calculated and delivered dose distributions can impact the probability of controlling the tumor or of avoiding normal tissue complications. This means that the entire radiation therapy process must be continually subjected to a multidisciplinary QA process. Members of this process include the radiation oncologists, radiation physicists, radiation therapists, and dosimetrists. Physicists are responsible, in particular, for commissioning and QA of the imaging modalities used for treatment planning (CT scanners, etc.), the treatment-planning systems, and the treatment machines (linacs, etc.).

### *QA of medical LINACs*

Table 11–2 indicates the frequency and tolerance requirements for some of the QA checks for medical linacs, taken from recommendations by the American Association of Physicists in Medicine (AAPM) Task Group 40 (Kutcher et al. 1994). Tests are carried out daily on systems for which changes in performance could seriously impact patient positioning (laser position), patient dose (machine output), or patient safety (emergency off-button, etc.). Monthly QA repeats some of these, and also checks functions that are less likely to change (such as linac light-field positioning) or would have less impact on the patient's treatment (e.g., couch coordinate indicators). Both daily and monthly checks for radiation output are constancy checks that compare the measured output with a pre-determined value. The measurement of absolute dose is more complex and time-consuming,

**Table 11–2.** Some of the QA checks recommended by the American Association of Physicists in Medicine.

Test	Frequency	Tolerance
X-ray output constancy	Daily/monthly/yearly	3%/2%/2%
Electron output constancy	Daily/monthly/yearly	3%/2%/2%
Laser position	Daily	2mm
Door interlocks	Daily	Functional
Photon/electron beam energy check	Monthly	2%
Field size	Monthly	2 mm
Cross-hair centering	Monthly	2 mm diameter
Gantry/collimator angle indicators	Monthly	1 deg
Coincidence of all rotational axis with isocenter	Yearly	2 mm diameter

and is only done yearly. Note, however, that many centers carry out these tests more frequently than suggested here.

### Absolute dosimetry

The most common method for obtaining routine absorbed dose measurements is by way of a clinical ionization chamber placed in a *phantom* (typically a tank of water). When the chamber is irradiated, the gas (air) inside it is ionized, and the total charge collected is correlated to the total absorbed dose. The exact relationship between charge and dose depends on the design and manufacture of the chamber and the type and energy spectrum of the radiation (Almond et al. 1999).

Specifics of the manufacture of the clinical chamber are removed from the picture, however, by comparing it against a standard *calibration chamber* that has itself been calibrated against a national standard [such as the one at the National Institute of Science and Technology (NIST), near Washington, DC]. The electrometer to which the ion chamber is connected is similarly calibrated.

Several other factors have to be corrected for in the clinic. The ion chamber calibration is for a standard radiation source, cobalt-60, so that when it is irradiated by a linac, the output must be adjusted to account for the different energy spectrum. Similarly, the chamber reading (charge) must also be corrected for ion recombination, which depends on whether the beam is continuous, as in Co-60 units, or pulsed, as with medical linacs. Polarity effects (e.g., the difference in the signal when the chamber is at  $-300\text{V}$  or at  $+300\text{V}$ ) also matter. And finally, the reading is shifted, in a predictable way, by temperature and pressure variations, which affect the mass of gas irradiated in the chamber (which is open to the air).

Because of the time needed, absolute dose measurements with the calibration chamber are typically carried out only when the machine is first delivered, and then yearly after that, or when significant changes are made to the machine. When the machine is first installed, base values are established for the clinical ion chambers and other radiation

detectors for simpler, more frequent (daily, weekly, monthly) output checks. These should be plotted, of course, to reveal any signs of drift or jumps in readings.

Although ion chambers are the most common detector used for calibration and other QA checks, they are not suitable for all dosimetry needs, and the physicist has a number of other dosimeters with they can use, including diodes, thermoluminescent dosimeters (TLDs), and metal oxide semiconductors-field effect transistor (MOSFETs).

## 11.3 Treatment Planning Processes and Tools

The general issues and processes of treatment planning were discussed in section 11.2. Here we describe some of the specific treatment planning processes and tools employed in a modern cancer treatment facility—in particular, treatment simulation, the use of multiple imaging modalities, dose calculations, treatment planning optimization tools, and IMRT.

### 11.3.1 Treatment Simulation

The purpose of simulation of a patient is to assist in designing the specific set of beams that will be adopted in treatment. It requires decisions on the number of radiation beams needed, the gantry and collimator angles for each beam, and any additional blocking needed to protect sensitive tissues.

There are two main types of treatment simulation: conventional and virtual.

#### Conventional simulation

A *conventional treatment simulator* is a diagnostic x-ray imaging machine that mimics the geometry of the treatment unit. In common with the linac, it consists of a gantry, collimation system, and patient couch, all of which have axes of rotation that meet at the isocenter. Instead of a MV therapeutic x-ray source, the simulator has a kV imaging x-ray tube mounted on the gantry, is equipped with a fluoroscopic x-ray imaging device [e.g., image intensifier plus charge-coupled device (CCD) camera], and can also take x-ray films.

Because the geometries are identical, any images taken during the simulation will show the treatment beam's-eye-view of the tissues that will be irradiated. The fluoroscopic detector is used to image the patient in real-time as the gantry rotation, collimator position, and patient couch position are adjusted in search of a clinically acceptable position and alignment of the first beam. An x-ray film is then taken by the simulator, and the radiation oncologist draws on it any attenuating beam blocks needed to protect certain healthy tissues (Figure 11–11). The same procedure is then repeated for the other treatment beams.

As with the treatment unit, the simulator has lasers that intersect at the isocenter. These are used for marking the patient with the tattoos that will be used for positioning the patient in preparation for the actual radiation treatments. Also, x-ray films shot in the treatment room can be compared with those taken in the conventional simulator to confirm proper setup.

Despite their long history of faithful service, conventional simulators have several important shortcomings. For one thing, with a few exceptions (e.g., lung cancers), it is usually not possible to visualize the tumor directly, and its position must be inferred from its presumed location relative to anatomic landmarks, such as bones. Also, no 3-D information is available, so it is not possible to draw 3-D volumes, such as GTV and CTV. Likewise, the simulation does not provide 3-D information about the tissue density variations (heterogeneities) that could (and perhaps should) be included

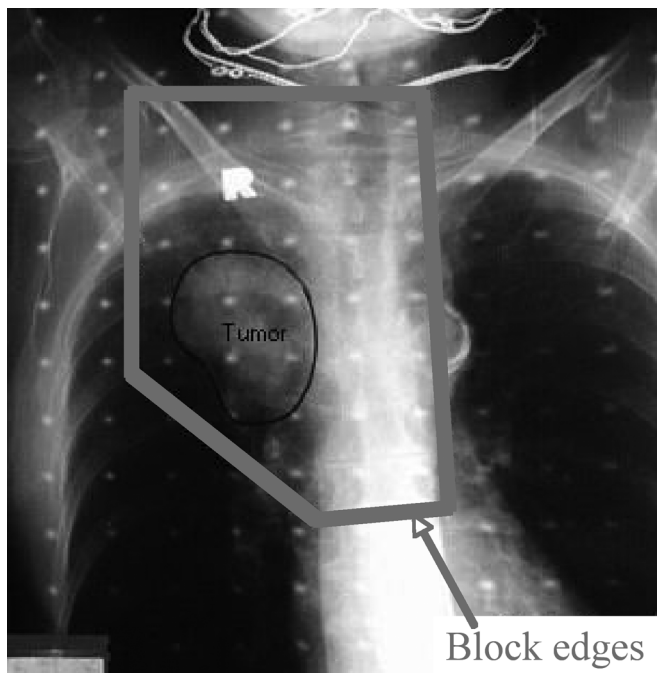


**Figure 11–11.** An x-ray film taken during a conventional simulation, showing the extent of the tumor and the radiation field as drawn by the radiation oncologist.

in the dose calculation. And finally, it is not possible to change beam angles after the simulation, and any significant modification of the plan requires re-simulation.

Fortunately these problems vanish with virtual simulation.

### *Virtual simulation*

Virtual simulation is a process that mimics conventional simulation by way of information from a 3-D imaging modality, typically CT, and special software.

Instead of the real patient, it works with a 3-D representation obtained from multiple CT slices from a slightly modified conventional CT scanner. One modification is that the patient table must have a flat surface, as with linac treatment tables. Also, immobilization and localization aids used for treatment must also be included in simulation; sometimes this necessitates the use of a wide-bore CT scanner, particularly when the patient will be treated with arms over the head. Likewise, the CT room should have positioning setup lasers identical to those in the treatment room to allow patient tattooing.

When the CT slice-images have been combined to create a 3-D representation, the virtual-simulation software can *calculate* beam's-eye-view images that should look just like the x-ray films taken on a conventional simulator. Once the isocenter, which is typically the center of the target volume, has been identified in the CT images, the patient can be marked, and then go home; structure delineation and beam placement can be decided later. Simple conventional conformal treatments can be planned almost entirely using virtual simulation.

Because this is a digital process, it is also possible to artificially enhance important anatomical structures. Also, here there are a variety of digital tools for the delineation of target structures, or registering the CT-generated images with those from other modalities such as PET or MRI. But somewhat strangely, virtual simulations systems have evolved so far with no dose calculation ability. So the simulation data, including the CT-based images, must be passed on to a separate treatment-planning system. This has limited the usefulness of virtual simulation systems in the planning of more complicated techniques, such as IMRT, but this shortcoming is sure to be remedied soon.

While nearly all treatment simulations carried out in modern cancer centers are virtual simulations, there are still some occasions when conventional simulation is appropriate and cost-effective.

### *Delineation of the target*

Delineation of the target and any other important structures is necessary for calculation of doses to these tissues, and is an important part of the virtual simulation process. This can be done automatically or freehand.

Most automatic delineation tools are based on some form of thresholding, requiring a tissue to have some range of

CT numbers, followed by post-processing to smooth, fill gaps, and remove outlying regions. More sophisticated tools are becoming available, and display varying degrees of usefulness and success, but their use is generally restricted to contouring the entire body (i.e., body vs. air), bone surfaces, the brain, lungs, and bladder.

Current practice is, therefore, to delineate the volumes manually, using freehand drawing tools to draw around the targets on axial CT slices, followed by some automatic data-processing on the contour sets. This, however, can lead to significant intra- and inter-user variations in both the interpretation and the delineation. Intra- and inter-user variations in spinal cord contours drawn by treatment planners (dosimetrists) have been found to vary by up to 7 and 9 mm, respectively, for example, and inter-user differences in contouring the esophagus are as much as 30 mm. And the dimensions of the primary tumor are reported to have an inter-user nonagreement of up to 73 mm (Collier, Burnett, and Amin 2004; de Steene, Linthout, and de Mey 2002).

Although such irregularities may introduce systematic major errors in treatment, or even lead to the treating of incorrect tissue volumes, the risk of missing some tumor tissue because of uncertainties in the delineation is reduced by accounting for the uncertainty in the expansion from GTV or CTV to PTV. Also, the primary target and other very important volumes are typically drawn by the radiation oncologist. The future improvement of automatic contouring algorithms is increasingly important as we use advanced techniques like intensity-modulated radiation therapy (see below), and try to escalate the dose to the tumor whilst still maintaining acceptable dose to critical structures.

### 11.3.2 Imaging Modalities Used in Treatment Planning

Virtual simulation and dose calculations are almost always based on CT. It is often useful to supplement the CT images with MRI or PET, both of which can provide additional information useful in identifying the target tissues (Buthiau et al. 2003).

#### *CT imaging*

CT imaging is the dominant modality used for 3-D dose planning. It is up to the job, and the equipment is relatively cheap and widely available. Also, CT images contain information on tissue electronic density needed for dose calculation, and they are relatively immune to artifacts or distortions (except those caused by high atomic number materials, such as teeth fillings and artificial limbs). Because soft tissues, muscular structures, and tumors can have very similar attenuation coefficients, however, it can be difficult or impossible to differentiate edema (swelling) or scar tissue from tumor. Although this was not a serious problem with traditional radiation therapy, with its relatively large fields, it does

become an issue with conformal therapy and, particularly, IMRT, when treatment margins are reduced. Accurate delineation of the target and other structures is important if smaller margins are to be considered without the risk of missing some of the tumor.

#### *Magnetic resonance imaging*

Various MRI RF/gradient-pulse sequences can often delineate soft tissues, and differentiate benign from malignant tumors, more accurately than can CT, and with less inter-user variations. Prostate target volumes selected with MRI, for example, are typically smaller than those of CT by around 10%, allowing a reduction in treatment volume and less dose to the rectum and bladder. Likewise, high-grade gliomas are infiltrative tumors with margins that are difficult to differentiate on CT, meaning that some of the tumor may be missed, so physicians tend to be generous in their contouring of the target (to kill the tumor); but the use of MRI here, too, can help delineate the tumor more accurately, thereby allowing less planned dose to surrounding normal brain tissues.

#### *PET and SPECT*

The increased glucose metabolism of cancer cells compared with normal tissue means that PET with F-18 fluorodeoxyglucose (FDG) can also be very useful revealing tumors. In many cases this can allow a reduction in planned dose to normal structures. This is particularly useful in cancers in the thoracic region, such as thoracic lymphomas, as lung radiation damage is strongly correlated to the mean dose.

SPECT can also be useful in differentiating cancer and normal tissues, such as with neuroblastoma. Similarly, SPECT lung perfusion scans can also be used to give a quantitative assessment of the functional condition of different parts of the lung, which may be important in deciding which sections of lung to avoid in lung tumor treatments.

#### *Image fusion*

Although MRI, PET, and SPECT all provide information useful for radiation therapy planning, only CT can give the high-resolution images with accurate external contours and electronic density distribution needed for accurate dose calculations. This means that the final radiation treatment plan is nearly always based on CT. A qualitative comparison of diagnostic MRI or PET images with the CT image used for treatment planning will allow some improvement in the delineation of tumors, but much more accurate results are possible if the images are registered together, so that the position of each voxel in the MRI or PET image is co-registered with a voxel in the CT image. This has been problematic in the past, but now most virtual simulation and treatment-planning systems have the necessary functions for manual or semiautomatic co-registration of multi-modality images. The clinical use of these modalities in radiation therapy planning has increased in the

last few years, and some large radiation oncology departments have bought their own MRI and CT-PET fusion systems.

### 11.3.3 Dose Calculations

After the virtual simulation, the beam-parameter data are transferred to a treatment-planning system, where dose distributions are calculated. We will only discuss photon beam algorithms, but many of the basic concepts and trends also apply to electron beam and brachytherapy algorithms. The three broad categories of dose calculation algorithm are data-driven algorithms, model-driven algorithms, and Monte Carlo calculations (Prado and Prado 2004; Papanikolaou et al. 2004).

Task Group 53 of the AAPM suggests that dose calculations should be accurate to within 0.5% to 1.0% for the center of simple fields in homogeneous media (e.g., water), to 3% to 5% in the presence of complicated heterogeneities. Doses should be accurate 2% to 7% in the beam penumbra, and 20% to 50% in the build-up region (which has very steep gradients over short distances, and is difficult to model).

#### *Data-driven dose calculation algorithms*

*Data-driven algorithms* calculate dose directly from experimental beam data (depth-dose curves, dose profiles, etc.). The data are usually obtained with ion chambers in tanks of water for a range of treatment energies and field sizes. Because it is unrealistic to collect raw data for every possible treatment scenario, and because water tanks differ somewhat from real patients (including the presence of density heterogeneities), data-driven algorithms use interpolation and correction factors to account for these differences. This means that although they can be accurate for simple plans, they are less so for complicated field shapes or patient geometries.

#### *Model-driven dose calculation algorithms*

*Model-driven algorithms* employ mathematical equations to describe the entire radiation transport process. Because this approach is based on the physics of the radiation transport process, the dose calculations can be very accurate, even for scenarios very different to those used for the initial verification set, such as those including off-axis heterogeneities and unusual field shapes.

An example found in several commercial treatment-planning systems is the convolution superposition algorithm. One implementation of this algorithm calculates the deposited dose in four stages.

First, it calculates the energy fluence exiting the linac. It starts with a uniform plane of energy fluence, and then adjusts this to account for the variations in the beam profile caused by the flattening filter, off-axis scatter, geometric penumbra (focal spot size), transmission through blocks or

MLCs, and the transmission and beam hardening effects of wedges and other beam modifiers.

It then projects the energy fluence through a 3-D representation (e.g., CT image) of the patient, using ray-tracing, and calculates *Total Energy Released per unit Mass (TERMA)* for each voxel. This calculation uses mass-attenuation coefficients (related to CT number), which are stored as a function of density, radiological depth (to account for beam hardening), and off-axis angle (to account for off-axis softening of the spectrum).

The third step calls for a superposition of the TERMA in a volume with an energy deposition kernel to compute the spread of energy (in the form of scattered photons and electrons) from the primary interaction site, giving a 3-D dose distribution. Again, this is done using a ray-tracing technique accounting for radiological distance (heterogeneities). The kernels are obtained in separate Monte Carlo calculations.

And finally, the effect of electron contamination (electrons from the linac collimators) is taken into account.

The implementation of this algorithm by one manufacturer involves more than 30 adjustable parameters to fully describe the photon fluence for a single nominal photon energy: 16 to describe the spectrum, 4 for the in-air fluence, 3 for head scatter, 2 for source size, and 8 for electron contamination. All of them must be systematically adjusted for an individual treatment machine until calculated and measured doses match within acceptable limits (1% to 2%).

Model-based algorithms are, of course, only as good as the original model, and compromises are often made to reduce calculation time. There are several clinical situations where the calculations are known to be less reliable, particularly at sites with significant inhomogeneities, such as the head/neck region, lung, breast/chestwall. These treatment scenarios can be modeled reliably only with a Monte Carlo approach.

#### *Monte Carlo dose calculation algorithms*

*Monte Carlo dose calculations* use the known physics of particle interactions to simulate the paths of individual particles (photons, electrons, etc.), first within the linac's head and then within the patient. Millions or billions of hypothetical photons (for an x-ray treatment) in a beam are directed at the treatment field. For each incident photon, and for every scatter photon thereafter, photon-electron interactions are then decided randomly based on known probabilities. Likewise, the Coulombic collision of every secondary Compton electron and delta ray with tissue atoms, down to the very last photo-electron, is followed mathematically. Monte Carlo calculations can obviously be extremely intensive computationally, and they are not yet ready for routine clinical application, but they do have the potential to be much more accurate than the others.

The Monte Carlo simulation can be carried out in three stages. The first models the inner accelerator head, including

the target, primary collimator, and filters. This stage produces a phase-space, which details the type, energy, position, and direction for all particles leaving the head. The large numbers of electron interactions and absorption of photons in the accelerator head means this stage is very computationally intensive. But because this calculation is independent of patient geometry, field size, etc., it usually needs to be carried out only once.

Then the beam modifying devices such as secondary collimators, blocks, MLCs, wedges, and other compensators are modeled. This is treatment specific, and also requires heavy-duty number crunching.

In the final stage, transport within the patient, as represented by a CT image, is calculated. CT images typically have 1-mm voxels, small compared with the photon mean free path. This generally demands a long computation time, especially around regions where there may be heterogeneous tissue interfaces, where the voxel size may be set to even less than 1 mm so as to obtain more accurate dose values.

The main advantage of Monte Carlo simulation is in the presence of large or complex heterogeneities where electronic equilibrium is complex and standard algorithms are less accurate. The general trend is now away from data-driven algorithms and towards Monte Carlo algorithms. Currently, most treatment-planning systems use model-based algorithms (or are changing to these algorithms). Some vendors currently do offer Monte Carlo modules.

#### 11.3.4 Treatment Planning Optimization Tools

The standard beam configurations used in radiation therapy were described in section 11.2. Much of that kind of work has traditionally been carried out by a dosimetrist, who manipulates beam weighting, blocking and wedging, etc., manually in an iterative fashion, searching for a clinically acceptable plan. Now, by contrast, there is a strong effort to continue the development of computer-based optimization techniques that can find plans to maximize the therapeutic ratio for radiation therapy treatment plans automatically. A more theoretical approach may be found in (Wolbarst et al. 2006).

##### *Field-in-field techniques*

Field-in-field treatment planning is a technique that uses multiple static fields of different sizes to achieve good homogeneous dose distributions without the need for wedges or other beam modifiers. The approach is particularly useful for the breast, but is applicable also to other sites. The process begins with creation of an open-beam plan, with MLCs blocking any critical structures, and calculates the dose distribution, keeping watch for hotspots. Next, it designs a subfield with the MLCs closed to block the hotspots; again it calculates the dose distribution, and weights the subfield to reduce the hotspot doses. It repeats this process iteratively,

until an acceptable plan is achieved. A particularly useful tool when planning a field-in-field treatment is the option to view 3-D dose clouds (iso-surfaces) from a beam's-eye-view, as this allows the user to block the beam above the dose hotspot (e.g., 110%) and thus reduce the number of x-rays reaching this region. The resulting x-ray intensity distributions are more customized than if wedges were used, so field-in-field techniques can offer improvements in homogeneity.

##### *Dose boosting techniques*

*Dose boosting* techniques increase the therapeutic ratio based on the rationale that subclinical microscopic disease can be controlled with a lower dose than needed for the gross tumor. First a large volume is irradiated, then a smaller volume containing only the primary tumor is taken to a higher dose.

Electrons are often used for dose boosting, particularly for superficial scar tissue, or for cases when there are critical structures (like the spinal cord) a short distance below the treatment volume. Instead of treating a smaller volume to a higher dose after the main treatment is completed, it is possible to plan treatments to give higher daily fractions to some regions than to others. For example, in a head and neck IMRT plan, various regions may be simultaneously treated to 2.0 Gy, 1.8 Gy, and 1.7 Gy per day over 35 fractions to give total doses of 70 Gy, 64 Gy, and 60 Gy, respectively.

#### 11.3.5 Intensity-Modulated Radiation Therapy (IMRT) Planning

Planning for IMRT is quite different from that for conventional conformal therapy (Ezzell et al. 2003; Waldron 2003). There are typically many more fields, and more gantry angles. Most planning for IMRT is inverse-planned, meaning that the user identifies the required dose distribution, and then uses automatic algorithms to try to find the treatment fields that can achieve this as well as possible. And the dose calculation itself is more challenging for IMRT than for conventional treatments, involving numerous small fields.

The delivery of IMRT also can be extremely complicated if the MLCs are moving during the treatment. The extra complexity of IMRT treatments compared with conventional treatments means that at most centers that employ the technique, an experimental evaluation of the delivered dose is carried out for each plan before the patient treatment commences. This is done using ion chamber and film placed in a solid water (a material that has the same MV x-ray properties as the real thing) to measure absolute dose at a point and relative dose distribution, respectively.

##### *The optimization process*

The first step in the optimization process is to determine the clinical goals. In nearly all IMRT-planning systems these are

defined in terms of dose-volume limits; in the future, the use of dose-response limits based on biological models may become more widespread. For a target that must receive 60 Gy, for example, the oncologist might set a minimum requirement of 60 Gy throughout the target, and a maximum limit of 63 Gy (105%) to prevent excessive hotspots within it. The treatment planner would select the photon energy, number of beams, gantry angles, and couch angles—these could, in principle, be included in the optimization, but that would significantly increase the size and complexity of the computations involved; indeed, class solutions can be developed, where the same parameters and constraints, are always used for a given treatment site, subject to occasional small, patient-specific adjustments. For example, one clinic may always treat paranasal sinus tumors using nine gantry angles evenly spaced every 40°, 6 MV photons, and no couch rotation, and may treat prostate cancers using five gantry angles with 10 MV photons.

Each dose-volume constraint must also be assigned an importance factor. For example, if it is considered more important to kill the tumor than save the use of one kidney, then the target constraints would be given a higher importance factor than those given to the organ-at-risk. Very important constraints (such as the need not to sever the spinal cord) that are given very high importance factors can, in some systems, be labeled as a hard constraint that must be met. Once the constraints and importance factors have been assigned, the algorithm can calculate an objective function.

Many objective functions have been designed, but one which is fairly representative is the *dose-matching quadratic objective* function, which calculates the sum of the squares of the differences between the calculated and prescribed dose at various points (e.g., around/within the target boundary, and at certain locations throughout critical and other healthy tissues), weighted by the importance factors, subject to the pre-assigned constraints. A quadratic programming algorithm then searches for the fluence patterns that will give the minimum value for the objective function. *Gradient search algorithms* are fast but, if the objective function has local (not global) minima, they can become trapped. This problem can be overcome with stochastic techniques such as *simulated annealing*, which simulates the thermal annealing process, or with *genetic algorithms*, which can escape local minima. These methods are slow, however, and with gradient search techniques, the presence of local minima does not usually cause the generation of clinically unacceptable plans. In most cases, the optimization process is still iterative, with the user looking at the optimum plan found, and perhaps adjusting the constraints and re-optimizing; this is particularly true for complicated cases (like tumors in the head and neck), as the algorithm can often put dose in places that were not specifically given a dose constraint, but still should be protected.

### *Dose calculations for IMRT*

The calculation of dose distributions in IMRT can be particularly challenging. Treatment fields can be very small, meaning that radiation scattered out from the region-of-interest may not be matched by radiation scattered into the region, resulting in electronic nonequilibrium. By a like token, most fields are blocked for much of the beam-on time, meaning that the amount of dose due to x-rays that pass through or are scattered by the MLCs is not insignificant, and the impact of this should be included in the dose calculation. The effect of inhomogeneities and irregular surfaces can also be significant.

Accurate inclusion of these factors in the dose calculation would increase the calculation time significantly. In conventional planning, calculation time is not a crucial factor, as the dose distribution is typically computed only once. In inverse-planned IMRT, however, the dose distribution may be calculated hundreds (gradient-search methods), or even hundreds of thousands (simulated annealing methods) of times, before an optimal plan is found, which means that the speed of the algorithm is extremely important. Many treatment-planning systems therefore use an approximate dose calculation during the optimization process:

Typically, a preliminary, *pencil-beam model* is used (data-based algorithm), which ignores off-axis heterogeneities, is averaged over energy, and assumes that the narrow pencil beam is normally incident on the patient surface. The algorithm is further speeded up by calculating dose for only a limited number of points, and by ignoring delivery limitations, such as MLC position limitations, during the optimization process. Once the optimal (often called the “ideal”) fluence is found in this manner, the parameters describing it are transferred to the full treatment-planning program, which proceeds to calculate the final dose distribution with its more accurate algorithm (such as the convolution/superposition algorithm). In many cases, this “final” dose distribution is not as good as the ideal fluence calculated with the less accurate, pencil-beam algorithm, which did not include the effect of the MLCs or other factors, and it may be advantageous to re-optimize using different dose constraints.

As computer speeds increase, there will be less need for these compromises in the dose-calculation engine. It seems likely, however, that this basic methodology of only calculating a very accurate dose distribution at the end of the optimization will be retained by most manufacturers for the foreseeable future. Some large centers already calculate a final dose distribution with in-house Monte Carlo programs, and at least one commercial Monte Carlo dose calculation system has become available.

## **11.4 Treatment Delivery Processes and Tools**

Here we discuss in more detail some important aspects of the actual treatment, beginning with standard treatment delivery

machines, including the verification and localization issues faced when setting up the patient. Also covered will be specifics of IMRT and stereotactic techniques.

#### 11.4.1 Description of a Medical Linear Accelerator

Although treatment units with Co-60 as the radiation source were common in the past, these days nearly all electron and x-ray radiation therapy treatments are carried out using a microwave-powered electron linear accelerator (Figure 11–12). An electron gun injects pulses of electrons into the waveguide structure that accelerates the electrons to high energy. The acceleration structure consists of a linear array of microwave cavities connected in series by central openings; these are arranged to couple the 3-GHz microwave power, produced by a magnetron or klystron, into the cavities in such a way that the resulting electric fields will accelerate the bunches of electrons.<sup>1</sup>

Low-energy medical linacs (4 to 6 MV) have short waveguides, which can be aimed at the treatment isocenter. Because of space requirements, the longer waveguides of higher energy machines are aligned parallel to the floor; magnets must be used to bend their path towards the treatment isocenter. Because 90° bending magnets can result in an energy-dispersed beam, the electron beam is usually bent through 270° (Khan 1994; Green and Williams 1997; Karzmark and Morton 1998).

#### Treatment head

What happens to the high-energy electrons once they leave the waveguide depends on whether the linac is producing

<sup>1</sup>A magnetron is a high-power oscillator that generates several hundred microwave pulses per second, each with a duration of several microseconds. A klystron is a microwave amplifier that requires a low-level microwave source, but is capable of much higher power and stability than magnetrons. Typically, magnetrons are used for low-energy linacs (4 to 6 MV), and klystrons are used for high-energy machines (18 to 20 MV).

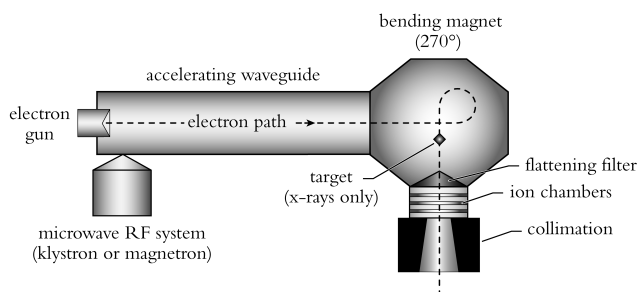


**Figure 11–12.** Microwave-powered linac. Bursts of electrons from the gun are accelerated to very high velocity in the waveguide, into which microwave energy from a klystron or magnetron is fed. After being re-directed by the bending magnet, the electrons either crash into a tungsten target to create bremsstrahlung x-ray radiation, or are scattered by a thin metal foil to produce a reasonably flat electron treatment beam.

photon or electron beams. If the accelerated electrons are being used to produce x-rays, a tungsten target is moved into their path, leading to the generation of bremsstrahlung x-rays. The x-ray beam then passes through the target and the flattening filter, which uses a combination of attenuation and scattering to yield a radiation beam that is essentially flat across its central area. The final x-ray beam displays the well-known bremsstrahlung spectrum, with mean energy about one-third of the nominal peak energy.

For a therapeutic electron beam, the x-ray producing target is replaced with one or more metal foils in series, which scatter the incident thin line of high-velocity electrons and transform it to an almost mono-energetic, nearly flat, wide-area beam.

#### Output monitoring

Then the photon or electron therapy beam passes through a dosimetry monitoring system. An ion chamber with segmented electrodes can monitor not only radiation output (total and dose-rate), but also beam symmetry. If any of these parameters are outside permitted limits, then the control system will activate a hardware interlock, turning the beam off. A secondary ion chamber will trigger a backup interlock if the first chamber fails.

#### Field collimation

The photon or electron radiation is collimated by means of two pairs of moveable collimators (“jaws”), blocks of tungsten about 8 cm thick, that define the area of the radiation field. Below the jaws, various accessories can be mounted:

- *The MLC system.* In some designs, one of the linac’s own collimator pairs is replaced with MLCs
- Wedges and lead-alloy blocks to sculpt and shape the radiation beam
- Electron collimator systems, known as applicators, for electron beams.

#### Computer control of medical linacs

As the complexity of radiation treatments has increased, so also has the use of computers for linac control. The design philosophy for modern computer-controlled treatment machines was strongly influenced by large accidental overdoses delivered to several patients between 1995 and 1997. Faulty software design and an over-reliance on software control and monitoring were partly responsible, along with a lack of hardware-implemented safety interlocks. Since these incidents, linac manufacturers have taken the approach of maintaining basic hardware monitoring and control, and using computer control in parallel with, or in addition to, this. Patient safety is ensured by hardware interlocks that prevent the beam being turned on if dosimetric or safety errors

occur, irrespective of the computer control. The design of the computer-control systems varies between linac manufacturers, but there are several important elements that they share. The timing of computer events is monitored, and a hardware interlock is triggered if any computer events are late, such as might be caused by a communications error. Also, the control system can only be in one state of control, such as “setup,” “beam on,” or “normal terminate” at a time, and the transitions among them are monitored, with an interlock triggered if any occur improperly.

#### 11.4.2 Localization and Verification Issues

Geometric imprecision and variability in treatment delivery can cause differences between the planned dose distributions and those that are delivered. One primary cause of these is systematic or random irregularities arising in simulation and/or treatment setup. (The distinction between the two is often blurred, as any random error occurring in the planning process will appear as a systematic problem in the treatment process for a given patient in all treatment fractions.) Systematic positioning errors might arise because the lasers and other marking devices used in the treatment or simulation might not be perfectly co-aligned. Alternatively, the patient may have been tense during the simulation and skin tattooing, but more relaxed after becoming used to the treatment routine. Likewise, internal organs such as the prostate may move around significantly (Langen and Jones 2001), so it is unlikely that a single CT image used during planning would reflect the average position, but rather may well represent one of the extremes; even if the simulation did capture the average position spot on, the organ might not be near it during any particular treatment—one source of purely random error. So, too, are inter-therapist variations in patient setup and daily motions of the internal organs. There may also be “sliding systematic variations” such as a slow shift in location of the target or a critical organ as the patient loses weight as the treatment progresses or a change in the tumor size as cancer cells are destroyed.

Some systematic and random uncertainties can often be reduced if daily imaging is used to correct patient position immediately before each fraction is delivered. But with a few exceptions, like prostate IMRT, the gains in setup precision are generally not considered sufficient to introduce time-consuming daily imaging into routine clinical practice.

If internal organ motion is small, as for tumors in the head and neck region, the systematic component can be removed making use of orthogonal images taken the first day of treatment. When the motion tends to be larger, it is sometimes possible to calculate the systematic error based on images from the first week or so of treatment, and then to apply the calculated position shift for the rest of the patient’s treatment. Random setup uncertainties do remain, of course, and an important way to reduce them is with good immobilization and localization devices.

#### *Immobilization and localization devices*

The purpose of these devices is to position the patient in the same way as during the simulation, and also to immobilize him or her so as to not move during the treatment (Bentel 1996). The device establishes the relationship between the patient coordinate system and the room coordinate system, so its alignment with the room system must be accurate and reproducible; usually this is done by aligning marks on the device with the room lasers, but attaching it to the patient couch at indexed positions can also be used. Any immobilization systems should be comfortable, of course, to reduce the tendency for the patient to move.

An additional role of some devices is to move normal tissues out of the radiation beams. By having the patient lie prone on a board with a hole in it for the patient’s belly, for example, it is possible to reduce the amount of intestine irradiated by the lateral fields. Positioning and immobilization devices have improved over the years, and it is now often possible to immobilize and localize the patient within several millimeters (Figure 11–13).

Once positioned, the position of the patient should be verified. Traditionally this is done using film, but electronic portal imaging devices (EPIDs) and other imaging modalities are becoming more common (see sections 11.4.3 and 11.5.2).

#### 11.4.3 Modern Devices

EPIDs and MLC assemblies are playing increasingly important roles in setup verification and radiation treatment delivery.

#### *MLCs*

MLCs are small, individually motorized collimators that can be used to shape or provide intensity modulation of the treatment field. They are now considered an essential part of a linac, and it is very unlikely that any modern radiation therapy center would install a new machine without MLCs. There are several basic configurations in which MLCs can be incorporated (Boyer et al. 2001):

One approach is to replace the upper jaw with two banks of MLCs, although a small backup jaw is retained. Because the leaves are relatively close to the x-ray source, they do not have to move large distances (the shape is magnified to the isocenter, and short leaves can be used, giving a compact linac head). The larger magnification compared to other configurations is also a disadvantage, however, as the leaves must be thinner, and the tolerances on leaf motion must be tighter, as any errors are also magnified. As a compromise, some manufacturers replace the lower jaws with MLCs instead.

An alternative is a *tertiary* system (Figure 11–14). Here the MLC device, consisting of two opposed banks of leaves, is positioned below the adjustable jaws of the treatment device, and it may be either permanently attached to the head or removable. This approach has the advantage that,

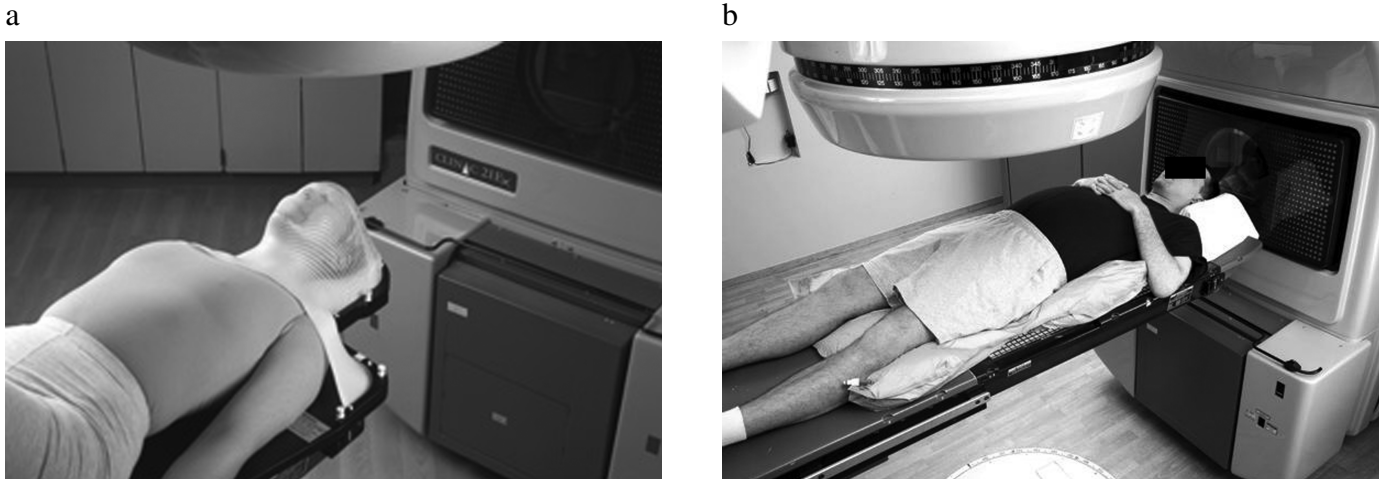


**Figure 11-13.** Some common positioning and immobilization devices. (a) An aquaplast mask and board attached to the patient couch, used for treating head and neck tumors. (b) Vac-Lok™ cushion molded around the patient to provide repeatable patient positioning for pelvic treatments. (Photographs courtesy of MedTec Inc., IA.)

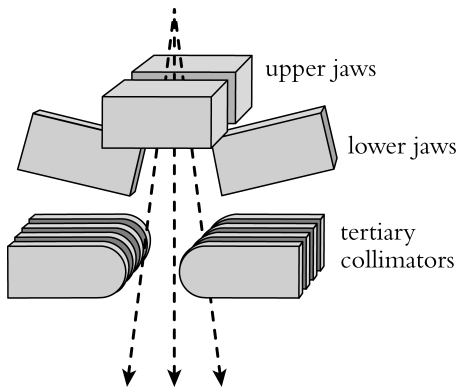


**Figure 11-14.** Tertiary multileaf collimator (MLC) system.

should the MLCs fail, they can be retracted out of the field-of-view, and simple treatments using the jaws or cerrobend blocks, are still possible. It adds to the size and weight of the gantry head, however, reducing the space available to position the patient.

A variation of the tertiary system, referred to as MIMiC™, is used for “rotating fan beam tomotherapy.” It inserts into the blocking tray of the linac head and collimates the x-ray field to a fan beam. MLCs from two rows are then either inserted into the beam to provide full attenuation, or retracted out of the beam. While most systems typically use linear screw bars to move the MLCs in and out of the beam, the MIMiC system employs pneumatic power. A MIMiC can be added to an existing linac, with virtually no downtime, but it is suitable only for IMRT, and cannot shape the fields for conformal therapy, as can other MLC systems.

When MLCs are being used to shape the radiation field, uncertainties in the leaf position of 1 to 2 mm may be acceptable, having no impact on radiation output or clinical out-

come. However, when the MLCs are used for IMRT (step-and-shoot or dynamic), positional accuracy and precision must be better than 1 mm. This is necessary because the radiation output for the individual small fields (often significantly less than 1 cm) used in IMRT can be strongly affected by small uncertainties in field size. Furthermore, in IMRT beam edges move to many positions, so uncertainties in MLC position may lead to the sum of the contributions from the many different edges adding incorrectly.

**Calibration and monitoring** of leaf position are clearly very important issues in MLC device design. Different manufacturers approach these in different ways, including:

- *Limit switches.* These can be used to detect leaf position for MIMiC MLCs, which only have an on or off state.
- *Linear encoders.* High-precision potentiometers, or similar devices, can give accurate positional readings for individual MLCs.
- *Video-optical systems.* A camera in the linac head can be used to detect the positions of the individual MLCs. By including reflectors in fixed positions in the head structure, this system can also be used for calibration.
- *Optical calibration.* The MLC device from at least one manufacturer has built-in narrow infrared beams that cross the paths of the MLCs. When the MLC is initialized, the system moves each MLC, one by one, across the beam. When the leaf blocks the beam, the values given by its positional encoders are recorded and used for calibration.

Backup position detection systems (e.g., two different linear encoders) are commonly employed so that the beam is terminated if the two systems do not agree sufficiently.

### EPIDs

Portal imaging is an important part of the patient setup verification process. This has traditionally been done with film, but there is a rapid movement to electronic portal imaging (Herman et al. 2001). The image reception, processing, and display stages are separate, as with any digital imaging modality, and can be optimized separately. Images are available immediately, so that the patient does not have to wait on the table while the image is being chemically processed; this reduces the chances of movement between the image being taken and the treatment beginning, and it also improves patient throughput. Also, the portal images can be made available electronically to all concerned parties—such as the radiation oncologist, who can approve them from the office if the department is served by a *Picture Archiving and Communications System (PACS)*.

A number of EPID designs have been investigated over the past two decades, including matrix-ion chambers and mirror camera-based systems, but they were not well integrated into the clinic workflow, largely because of poor image quality. The situation was so bad, in fact, that an informal AAPM survey in 2001 found that one-quarter of institutions that had installed EPIDS had actually given up using them. Recent development of amorphous silicon (a-Si) flat-panel array image receptors, better integration of the devices into department R&V databases, and the general increase of image-guided radiation therapy techniques have allowed many clinics to go totally digital, however, and we can expect the use of EPIDs to increase significantly in the future.

Most clinics still rely on special film for measuring dose distributions for QA purposes, including patient-specific QA for IMRT. But the trend will likely be towards the use of EPIDs for measuring 2-D dose distributions, as well as for patient verification.

**Design of EPIDs.** As with some devices employed in radiography and fluoroscopy (see chapter 1), EPIDs use a phosphor screen (usually gadolinium oxysulfide) to convert x-rays to light, and the light is immediately sensed by an adjacent optical-photon image receptor. Because they work with high-energy x-ray photons, however, the portal devices commonly also use some build-up material in front of the phosphor screen (as is sometimes done with bolus material if there is need to reduce skin-sparing for the patient), to improve the quantum efficiency. This is usually a 1 to 1.5 mm thick copper plate, but other materials, such as polyethylene, will also do. Electrons generated by x-ray interactions in the copper plate and phosphor screen produce optical photons in the

phosphor. These are then converted to charge by a photoelectric converter in an a-Si array, and the charge is stored in the pixel storage capacitor until readout. In spite of the copper build-up layer, the quantum efficiency (percentage of incident photons interacting with the detector) is still only around 2% (compared with 30% to 60% for diagnostic energy devices). A patient dose of 2 to 5 cGy is therefore necessary to give an image good enough for localization of bony structures; so two orthogonal images contribute some 5% of the daily prescription dose. If portals are only taken weekly, then this is low enough that it can probably be ignored, but if there is a need for daily images, then the extra dose must be accounted for in the dose prescription. Several research groups are working at improving the quantum efficiency, but the fundamental physics of imaging at high energy will make significant improvements difficult.

### 11.4.4 IMRT Delivery

As mentioned above, IMRT planning is carried out in several stages, with the optimization process usually producing an ideal fluence map that is independent of the exact method of delivery. The actual IMRT delivery can be achieved in a number of ways, including physical modulator IMRT, conventional MLC IMRT, rotating beam IMRT, and robotic linac IMRT (Ezzell et al. 2003).

#### *Rotating fan beams*

The first IMRT delivery technique to be widely commercially available was a rotating fan beam system, where one narrow pancake slice (2 or 4 cm) of the patient at a time was irradiated as the gantry rotated. The radiation intensity was modulated by collimator leaves that moved in and out of the beam. A newer system with a similar concept is tomotherapy (section 11.5.2).

#### *Physical modulator IMRT*

In physical modulator IMRT, the x-ray fluence is modulated using a filter positioned immediately below the linac head. This thickness of the filter is calculated from the ideal fluence map and fabricated on a patient-by-patient basis. Although this delivery technique may have a few advantages over MLC, it is really a transitory technology, and its use is rare.

#### *Conventional MLC IMRT: segmental and dynamic*

Nearly all IMRT carried out in modern institutions is conventional MLC IMRT, and there are two general approaches to it. With the simpler, called segmental MLC (SMLC) IMRT, the radiation fluence is delivered as a series of different shaped segments. The MLC leaves move to form the field shape for each segment, and the radiation is only turned on once the leaves are in their preset positions. There can be 30 or more segments for each gantry angle. The alternative approach, dynamic MLC (DMLC) IMRT, leaves the radiation

beam on as the MLCs sweep across the field, with their exact positions and speed controlled by computer.

Either way, it is necessary to use leaf-sequencing algorithms to find the sequence of MLC positions that will give a deliverable fluence that is very close to the ideal fluence, while also minimizing the total monitor units (MUs). Minimizing the MUs shortens the treatment time and also, and more significantly, reduces the amount of leakage radiation from the linac head, which reaches tissues distant from the treatment site.

Helical tomotherapy and robotic IMRT have only become commercially available relatively recently, and will probably see increased use over the next few years.

#### 11.4.5 Stereotactic Radiosurgery

Traditional *stereotactic radiosurgery (SRS)* is the treatment of intracranial lesions in a single fraction, using a dose of up to 20 Gy, ten times higher than for the fractions in a conventional fractionated treatment (Schell et al. 1995). The requirements for accuracy and precision are much higher than for the fractionated treatments in *stereotactic radiation therapy (SRT)*.<sup>2</sup>

##### Basic requirements for SRS

The basic requirements of an SRS system are:

- *Accurate localization.* Typically this is achieved by fixing a stereotactic frame rigidly to the patient's skull, which in turn attaches to the patient couch during both simulation (CT or MRI) and treatment. The target is delineated, and the treatment planned, with all points referenced to the coordinates of the frame. For SRT (i.e., fractionated) procedures, less invasive frames are used to provide the reference coordinates. Some systems also include portal imaging for setup verification. One manufacturer has even installed two x-ray tubes and two digital x-ray imaging devices on the treatment machine, so that stereo images can be taken and registered with the planning CT immediately before treatment.
- *Mechanical precision.* The stereotactic frame must be accurately aligned with the linac coordinate system. The isocenter should be very stable (i.e., its position should not change when the couch, gantry, or collimator is rotated), and this must be tested daily. Typically, the accuracy demand is better than 1 mm.
- *Accurate dose distribution.* SRS typically uses no PTV expansion, which means that the planned dose must be very accurate.

- *Patient safety.* In common with all treatments, patient safety is paramount. The high doses associated with SRS, and the complete lack of possibility of corrective action, mean that patient-specific QA and redundant checks of all stages of the planning and treatment delivery process are critical.

##### SRS treatment delivery systems

The two main delivery platforms for stereotactic irradiation are the gamma knife and the linac in an SRS configuration:

- *Gamma knife.* Much of the pioneering work in radiosurgery was carried out with the gamma knife. The most recent version consists of 201 Co-60 sources, each with an activity of around 30 curies, arranged in a hemispherical array aimed at the isocenter(s), which is near or at the center of the tumor. In addition to the primary collimation inherent in the irradiation unit for each source, secondary collimation is achieved using four helmets, which have different size collimator holes (4 to 18 mm). The desired dose distribution is achieved by using different helmets, by plugging different channels, and by treating multiple isocenters. The accuracy of dose delivery is better than 0.3 mm. At the time of writing there are 173 gamma knife units in clinical operation.
- *Linac stereotactic radiosurgery.* Most SRS is carried out using a linac, often using four to six non-coplanar arcs to give a concentrated dose to the target, while minimizing dose to surrounding tissues. Although the use of small MLCs for SRS/SRT is increasing, most procedures use special applicators that attach to the linac head. Different applicators are used for a range of diameter radiation fields. One manufacturer has attached a small accelerator to a robotic arm, offering a high degree of flexibility in delivering small beams under image guidance.

## 11.5 Recent Developments and Trends

We have introduced the main issues and processes in radiation therapy, and discussed how some of these are approached in modern radiation therapy centers. Here we will describe developments in medical physics that have either recently started to impact clinical practice or which we expect will do so soon, particularly in high-profile large centers. IMRT is not discussed below, as it is already considered a routine clinical procedure. IMRT optimization routines will be slowly improved (probably to eventually include gantry angle and collimator angle and biological optimization), as will the contouring and other routines that will improve speed and workflow in treatment planning and delivery. We concentrate,

<sup>2</sup>SRT is used when the risks of SRS are considered too high, but the high accuracy and precision of SRS is still considered useful. As an extension, similar techniques are used for extracranial sites such as spine, lung, and liver lesions.

rather, on the increasing use of imaging modalities in the treatment room, tomotherapy, adaptive radiation therapy, correction for intrafraction motion, and biological modeling.

### 11.5.1 Use of Imaging Modalities in the Treatment Room

The traditional patient setup technique of aligning skin marks with room lasers cannot match the accuracy with which radiation treatments can now be planned and delivered. The main problems with skin marks are that often only three of them are used, and also that the skin is flexible, meaning that setup uncertainty can be significant. Cameras in the simulation and treatment rooms might take 3-D images of the patient's skin surface, and use these to guide patient setup. But because the skin is not rigidly attached to the internal skeletal structure, and many organs move on an intra- or interfraction basis (Langen and Jones 2001), it is more effective to position the patient guided by imaging of the internal anatomy of the patient.

#### *Megavoltage x-ray imaging*

The use of electronic portal imaging for verification of the patient's setup, with the treatment machine used as the x-ray source, will continue to increase, particularly when good, reliable automatic image-fusion routines become integrated into the clinic workflow. As well as imaging for setup verification purposes, it is likely that EPIDs will soon be used for a number of other extremely important applications:

- *QA of IMRT fields.* The complexity of IMRT fields means that patient-specific QA is necessary before each treatment commences. Portal imaging devices can assess the fluence from the linac (without the patient present), which can then be compared with the expected outputs, and therefore used as pre-treatment QA.
- *Portal dosimetry.* In principle, it is possible to image the x-ray fluence that exits the patient and to use this to reconstruct the actually delivered x-ray fluence. If this were automated, such that it did not impact patient throughput, it could be used as a continual QA process that included the effect of the patient on the radiation beams.

#### *Kilovoltage x-ray imaging*

The low contrast and poor detector quantum efficiency of MV x-ray imaging can be overcome using kV x-ray tubes and diagnostic-type digital image receptors attached either to the gantry itself or to the treatment room ceiling/floor (as in one commercial SRS system). Several manufacturers have adopted the former approach, where the kV tube and detector are mounted perpendicular to the linac/EPID arrangement, but it may be some years before its use spreads beyond major cancer centers.

#### *Ultrasound imaging for target localization*

Ultrasound imaging devices designed specifically for radiation therapy are used primarily for localization of the prostate, but may also be applied to the liver and other sites. For one of these systems, the ultrasound probe is attached to a mobile cart by an articulated arm; the probe is inserted into a bracket attached to the linac gantry, thus establishing a geometrical relationship between the two devices. The patient is first set up using skin marks, and ultrasound images are then taken. Anatomical contours imported from the treatment-planning system are superimposed on the ultrasound images, and the therapist then shifts the contours from the two until they match (Figure 11–15). This shift is the distance by which the patient couch needs to be moved to correctly position the prostate for today's treatment. The ultrasound probe is then inserted into a second bracket attached to the patient couch, giving the relationship between the treatment machine, the ultrasound images, and the patient couch; software then monitors the position of the couch as the therapist moves it to the correct position. Automatic registration tools under development should improve accuracy and precision.

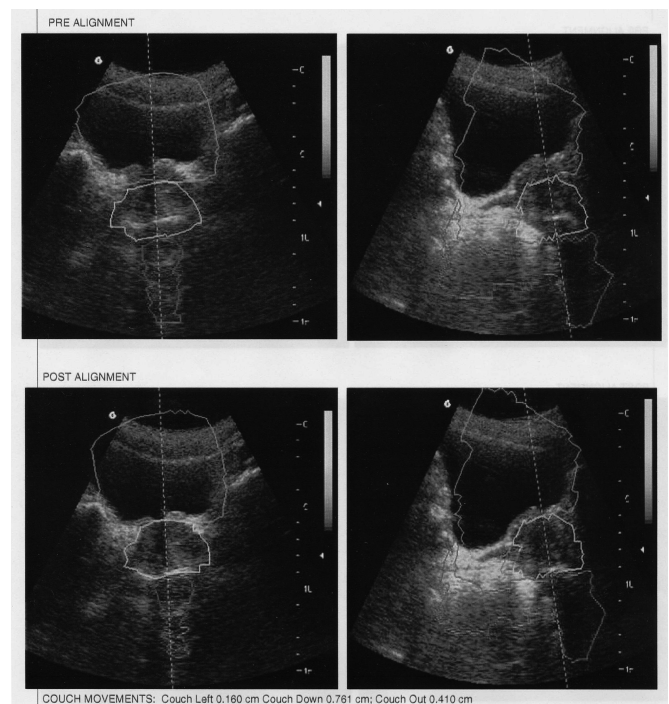


**Figure 11–15.** Ultrasound images of the prostate superimposed with the bladder, prostate, seminal vesicles, and rectum contours from the radiation treatment plan. The therapist first takes two ultrasound images (pre-alignment) and then manually shifts the prostate contour to match the images (post alignment). (Image courtesy of NOMOS Radiation Oncology Division, Cranberry Township, PA.)

Pros and cons: Such systems are inexpensive, portable, produce no ionizing radiation, and are reasonably simple to operate. The pictures can be noisy and difficult to interpret, however, and inter-user variations may be significant.

### *Daily CT imaging in the treatment room*

The only other imaging modality that can give soft-tissue discrimination, and is suitable for use in the treatment room is CT. The major manufacturers have been developing in-room CT imaging capabilities for some time, but these are still restricted to research centers.

The so-called “CT-on-rails<sup>TM</sup>” is designed and installed such that the coordinate system of the CT images is mechanically linked (by rotation of the treatment couch) to that of the linac (Figure 11–16) (Court et al. 2003). The patient is positioned on the couch, which is then rotated to the CT side. The CT gantry moves on rails past the stationary patient and acquires an image set.<sup>3</sup> (The dose from the CT is only 1% to 2% of that delivered to the tumor.) The couch is rotated to the linac side and, after the new images are compared with those of the treatment plan to calculate any necessary patient shifts, the patient can now be positioned exactly. Although CT-on-rails systems have been commercially available for a few years, their use has been restricted to research centers, and they are already being superseded by linacs with cone-beam CT capability. Because of the weight and mechanical design of a conventional linac gantry, a single 360° rotation takes around 1 minute, so multiple rotations to image multiple slices are not realistic (hence the use of CT-on-rails systems). This problem has been overcome with the introduction of fast and efficient large-area electronic imaging devices which permit the feasibility of cone-beam CT, which only

<sup>3</sup>With standard CT, by contrast, the gantry is stationary and the patient couch moves through the bore.

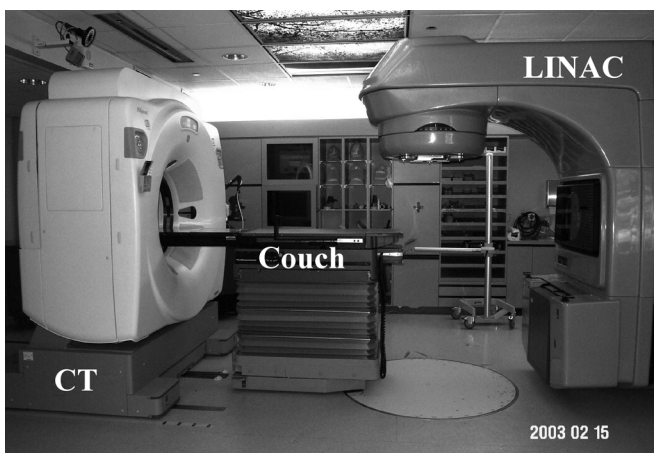


**Figure 11-16.** The CT-on-rails<sup>TM</sup> system at the University of Texas M.D. Anderson Cancer Center. (Image courtesy of Lei Dong, Ph.D.)

requires a single rotation of the x-ray source/detector around the patient.

Research centers are making good use of these new in-room CT imaging capabilities, and we will soon have some excellent data on interfractional motion of different tissues in the body. This might eventually be used to model shape changes that could then be included in the treatment-planning process.

### *The use of fiducials*

One way to overcome the inability to view most soft-tissue structures with transmission x-ray imaging is to implant radiopaque (typically gold) markers into the target, and perhaps elsewhere. Such markers, which may have rough surfaces to prevent them migrating through tissue, are easily seen on MV or kV images, allowing accurate localization. If fluoroscopic imaging is used, then real-time organ tracking becomes a possibility (see section 11.5.3), although this does require frequent x-ray exposure.

Alternatively, one can replace the radiopaque markers with magnetic transponders, detecting their positions with an external AC magnetic array; in principle, this allows continuous monitoring of the target position without the need for x-rays.

### 11.5.2 Tomotherapy

Linac gantries may be combined with CT systems to allow 3-D imaging immediately before treatment. The University of Wisconsin at Madison has pioneered the opposite approach, adapting spiral CT technology for a treatment machine (Mackie, Holmes, and Swerdloff 1993; Mackie et al. 2003). The system is built around a linac that is operated at 3.5 MeV during imaging, and 6 MV during radiation treatment. As in spiral CT, the rotation of the x-ray fan beam is synchronized with continuous longitudinal motion of the patient couch, giving a helical beam pattern. This is detected and used for reconstruction of the 3-D image; operation is similar thereafter, during patient treatment, but the fan beam is modulated using MLCs. Non-coplanar treatments (requiring several patient couch angles) are not possible, but the system is not limited by the slow gantry rotation speed, or gantry sag.

### 11.5.3 Adaptive Radiation Therapy

Current clinical practice is to plan radiation treatments using an image taken one or more weeks before treatment, with PTV margins decided based on clinical studies of the patient population. But as in-room imaging capabilities improve, so does the potential for adapting treatments to patient-specific characteristics (Yan et al. 1997; Vargan, Yan, and Kestin 2005).

Current PTVs are created by expanding CTVs by a margin that accounts for setup uncertainty and target random motion. For the prostate, random motion is caused by variations in rectal and bladder filling, and the extent of the motion is

known to vary significantly among patients. Daily in-room CT imaging for the first week of treatment can be used to assess the motion for a patient, and the treatment plan can be modified as appropriate: Patients with little random motion may be treated with smaller margins, reducing normal tissue toxicity, while those of patients with more than normal random motion would be increased to ensure sufficient target coverage.

Another clinical example for which adaptive radiation therapy may prove useful is with head and neck tumors, some of which can lose as much as 85% of their initial volume over the course of treatment. But tumor volume changes vary considerably among patients and cannot be predicted, so they cannot be accounted for in the initial treatment plan. In-room CT imaging, however, may provide data to evaluate what changes in the treatment, if any, are needed.

#### 11.5.4 Accounting for Intrafraction Motion in Treatment Planning and Delivery

Daily imaging of the patient before treatment makes possible the correction for any day-to-day variations in the position of the tumor or other organs (Langen and Jones 2001). But these can also move while the radiation beam is on (intrafraction motion). The diaphragm typically moves around 15 mm during normal breathing, for example, and parts of the liver, kidneys, and pancreas may travel a similar distance. Lung tumors can move more than 10 mm during respiration. Intrafraction motion can be accounted for in the treatment plan with increased treatment margins but, particularly for lungs, the risk of complication is correlated to the volume of normal tissue irradiated.

Also, many modern treatments, like dynamic IMRT, use moving beams or MLCs, which introduces the possibility for interplay between the motions of the organs and those of the beam. In an extreme case, a portion of the tumor might intermittently move out of the beam as the field changes although, for a fractionated treatment, this effect might partially average out over time. These are serious concerns, however, and it is important to be able to reduce, or measure and correct for, any intrafraction motion (Keall 2004; Murphy 2004; Mageras and Yorke 2004).

##### *Patient positioning*

The simplest approach is to position the patient such that respiratory motion does not affect the target organ. Breathing can cause the prostate to move by 5 mm or more for a patient in the prone position, for example, but there is virtually no motion of it for a supine patient.

##### *Breath-hold techniques*

Many patients can hold their breaths for 15 seconds or more, and the Deep Inspiration Breath Hold (DIBH) technique can reduce the intrafraction motion of thoracic tumors; a patient's breathing cycle is monitored using a spirometer or

other device, and the therapy beam is turned on when the patient reaches DIBH. Alternatively, it is possible to regulate breathing by actively controlling airflow through the spirometer. Either way, the CT image used for the treatment plan must be obtained using DIBH.

##### *Respiratory gating*

Respiratory-gated treatment monitors the patient's breathing and turns the radiation beam on for preset phases of the respiration cycle. Because it is carried out with the patient breathing normally, with no need for breath-hold, it may be less demanding and suitable to a wider range of patients. One technique developed for this purpose uses two x-ray tubes and fluoroscopic detectors to monitor the position of gold markers implanted in the tumor site. Radiation is turned on only when the position of the markers falls within some preset tolerance distance from the treatment isocenter.

The most common commercial method in the United States employs a video camera attached to a personal computer to monitor the position of infrared reflective markers placed on the patient's chest. As the patient breathes, the markers move up and down, giving a breathing waveform, which is displayed on a monitor. Control signals allow the radiation beam to be turned on only when the breathing waveform falls between two pre-set thresholds. If the patient's breathing becomes irregular, because of coughing, say, a periodicity filter algorithm turns the beam off until the patient's breathing is regular again.

##### *4-D radiation therapy*

Breath-hold and gating techniques are three-dimensional, in essence, as the aim is to freeze time stroboscopically. The next advance in correcting for intrafraction motion is to synchronize the radiation beam with the tumor motion. This technique, known as *4-D radiotherapy*, involves 4-D imaging (e.g., acquisition of a sequence of CT images over the breathing cycle); 4-D planning, with different plans calculated for different phases of the breathing cycle; and 4-D treatment, in which the 4-D plan is delivered over the breathing cycle.

The concept of 4-D CT imaging is fairly simple, and uses a conventional CT scanner. As the CT images are acquired, the patient's respiration is monitored using a spirometer, or any of the other devices mentioned above. Whereas in conventional CT imaging only one slice is taken for any longitudinal position, in 4-D CT imaging several slices are obtained at each, and labeled according to the detected respiration phase. After image acquisition is complete, the 2-D slices are re-sorted, based on their respiration phase, into a series of 3-D CT images. The final 4-D CT image set might consist of as many as 10 3-D CT image sets, each corresponding to a different phase of the breathing cycle.

This is a much larger amount of data than that for conventional planning, and the challenges of 4-D radiotherapy planning will be formidable. The first step in 4-D planning is to contour (segment) the target and critical organs for each phase. This is still normally done by hand, and the workload would increase by a factor of 10 or so with 4-D radiotherapy, clearly an unrealistic proposition; routine 4-D planning would have to rely on automatic deformable image registration algorithms, currently under development by several research groups. A treatment plan would then be calculated for each 3-D image set, and combined to give a 4-D treatment plan. Four-dimensional IMRT planning and treatment will prove to be even more difficult.

### 11.5.5 Biological Modeling

It is often necessary to compare two or more treatment plans; indeed, planning optimization, whether by a dosimetrist or an algorithm, consists of generating a range of possible trial plans, in essence, and picking out the one that best satisfies the treatment-selection criteria.

Comparison of competing plans is usually based on the examination of isodose distributions and DVHs, but it is often not clear from these which plans are superior (see Figure 11–9). An alternative method is to compute and compare biological indices such as tumor control probability (TCP) and normal tissue complication probability (NTCP) (Perez and Brady 1987). A tumor contains a large number of viable clonogenic cells, and it is commonly assumed that the local tumor is destroyed, and the patient is cured, only if none of these cells survive the fractionated treatment; TCP, a measure of the likelihood that treatment will bring this condition about, is calculated as the product of probabilities that individual clonogens are killed. Likewise, various forms of the NTCP indicate the probability of radiation causing damage to normal tissue.

One biological model that is widely used by both of them to describe the probability of cell survival after radiation exposure, largely because of its simplicity, is the *linear-quadratic survival curve (L-Q)*, introduced in the 1980s. The L-Q formalism acknowledges that for either normal or tumor cells, the main cause of lethal damage at low doses of low-LET (linear energy transfer) radiation is the double-strand DNA break caused by a single ionizing particle. (Single-strand breaks are much more common, but these are fairly efficiently repaired by the body.) The fraction of the cell population killed per unit of dose is independent of the dose already delivered,  $D$ , so the probability of a cell's escaping, surviving, this type of event,  $S_\alpha$ , is

$$S_\alpha = e^{-\alpha D} \quad (11.1a)$$

At higher doses, however, there is an increased probability of two separate ionizing particles working in tandem to produce

a lethal double-strand break; a cell's odds of surviving this type of event,  $S_\beta$ , are given by

$$S_\beta = e^{-\beta D^2} \quad (11.1b)$$

The overall probability of survival is given by the product of  $S_\alpha$  and  $S_\beta$ ,

$$S_{\alpha\beta} = e^{-(\alpha D + \beta D^2)} \quad (11.1c)$$

Damage can also be a function of dose-rate: Low dose-rates give more time for the repair of the single-strand breaks, thus reducing the amount of damage. This effect can be included in the model by multiplying a correction factor which is calculated based on the irradiation time for each exposure and the tissue repair rate (typically  $0.46 \text{ h}^{-1}$  for late-responding tissues, and  $0.46$  to  $1.4 \text{ h}^{-1}$  for tumors).

Because some tumors grow much faster than others, it may also be important to include cell repopulation in the biological model. This can be added to the L-Q formula, using the ratio of the overall irradiation time, and the tumor potential doubling time.

A strong feature of the L-Q model is that the sensitivity of specific tissues to different fractionation regimens can be quantified in terms of the  $\alpha/\beta$  ratio. Tissues that respond slowly to radiation, such as the spinal cord, brain, and eye, have curvy cell survival curves, low values of  $\alpha/\beta$  (typically 3 to 4), and high fractionation sensitivity. Quickly responding tissues, such as the skin, hair follicles, and testis, have straighter survival curves, higher  $\alpha/\beta$  ratios (around 8), and less fractionation sensitivity. With the  $\alpha/\beta$  ratio for the dose-limiting tissue, the L-Q model can help design and compare fractionation schemes. This can be useful if the clinical circumstances change, and the treatment regimen needs to be altered while maintaining the same biological effect. Similarly, the L-Q model can be used to compare low and high dose-rate brachytherapy treatments, and the dose-rate effect of using different permanent implants with different half-lives for brachytherapy treatments.

The L-Q is only one of many biological models, of course, and others have been exploited to publish tables on the biological effects during treatment of *Time, Dose, and Fractionation (TDF)*. TDF tables allow physicians or physicists to design alternative fractionated radiotherapy courses that will give the same biological effect. The credibility of the L-Q approach and TDF tables is supported by observations that their predictions tend to be consistent with clinical experience.

There is an important difference between the models used for TCP and NTCP. TCP is the probability of killing all the viable clonogenic cells in the tumor. Damage to normal tissue, however, is dependent not only on the dose, but also on the irradiated volume (hence the shape of the DVH).

There are several biological models that include this volume effect, including the LKB (Lyman Kutcher Burman) phenomenological model, which represents the NTCP as a function of four parameters: the tolerance dose for whole organ irradiation, the steepness of the dose response curve, a reference volume, and a factor to relate the tolerance dose for whole and partial organ irradiation. These parameters are estimated by fitting the LKB equations to clinical data for a given organ or tissue and for given irradiation conditions.

A few treatment-planning systems include radiobiological models for evaluating competing plans, but their use is somewhat controversial. First, the underlying models are fairly crude, and the parameters are not well known. Although it is possible to construct new fractionation schemes with the same probability of normal tissue complication, plan comparison is more complicated, and until better data are available, extreme care must be taken in adopting any model. The same is true if NTCP/TCP models are used for IMRT optimization, as errors in the probability estimates could force the search in the wrong direction. The fact that TCP is particularly sensitive to cold spots may, however, be useful in preventing these in IMRT optimizations.

Also, the models do not consider patient-to-patient differences in radiosensitivity (although this is true of most current treatment procedures, including dose-based prescriptions and choice of PTV margins). Current practice is to determine treatment for an individual so as to ensure a low probability of severe normal tissue complications, based on data for the whole patient population. This means that tolerance doses may be determined by the sensitivity of a (possible small) fraction of patients who are particularly sensitive to radiation. If they could be reliably identified, it may be possible to give higher doses to less-radiosensitive patients, thus increasing their TCP without a worsening in normal tissue complications. The development of accurate predictive assays of radiosensitivity is the subject of ongoing research.

## 11.6 Conclusions

We have described the major processes and tools for treatment planning and treatment delivery in radiation therapy. We also described some new developments and trends that are expected to influence this field over the next few years. Technologies that can be shown to help treatment planning or delivery without requiring a change in patient treatment protocols will see the fastest increase in use. These include multimodality imaging for both planning (particularly PET) and treatment verification (particularly electronic portal imaging). Technologies that include a change in the way the patient is actually treated will experience somewhat slower acceptance, including those that account for intrafraction motion, employ adaptive radiation therapy, or use radiobiological modeling. All these are active areas of research and development.

## 11.7 References

- Almond, P. R., P. J. Biggs, B. M. Coursey, W. F. Hanson, M. Saiful Huq, R. Nath, and D. W. O. Rogers. (1999). "AAPM's TG-51 protocol for clinical reference dosimetry of high-energy photon and electron beams." *Med Phys* 26:1847–1870. Also available as AAPM Report No. 67.
- Bentel, G. C. *Radiation Therapy Planning*. 2nd Edition. New York: McGraw-Hill, 1996.
- Boyer, A., P. Biggs, J. Galvin, E. Klein, T. LoSasso, D. Low, K. Mah, and C. Yu. AAPM Report No. 72. Basic Applications of Multileaf Collimators: Report of the AAPM Radiation Therapy Committee Task Group No. 50. Madison, WI: Medical Physics Publishing, 2001.
- Bushburg, J. T., J. A. Seibert, E. M. Leidholdt Jr., and J. M. Boone. *The Essential Physics of Medical Imaging*, 2nd Edition. Philadelphia: Lippincott Williams & Wilkins, 2002.
- Buthiau, D., O. Rixe, J. P. Spano, D. Nizri, M. Delgado, M. Gutierrez, J. Bloch, M.-A. Rocher, and D. Khayat. (2003). "New imaging techniques in oncology." *EJC Supplements* 1:28–42.
- Collier, D. C., S. S. C. Burnett, and M. Amin. (2004). "Assessment of consistency in contouring of normal-tissue anatomic structures." *J Appl Clin Med Phys* 4:17–24.
- Court, L., I. Rosen, R. Mohan, and L. Dong. (2003). "Evaluation of mechanical precision and alignment uncertainties for an integrated CT/LINAC system." *Med Phys* 30:1198–1210.
- de Steene, J. V., N. Linthout, and J. de Mey. (2002). "Definition of gross tumor volume in lung cancer: Inter-observer variability." *Radiother Oncol* 62:37–49.
- DeVita, V. T., S. Hellman, and S. A. Rosenberg (Eds.) *Cancer: Principles & Practice of Oncology, Vol. 1, 5th Edition*. Philadelphia, PA: Lippincott-Raven, 1997.
- Ezzell, G. A., J. M. Galvin, D. Low, J. R. Palta, I. Rosen, M. B. Sharpe, P. Xia, Y. Xiao, L. Xing, C. X. Yu. (2003). "Guidance document on delivery, treatment planning, and clinical implementation of IMRT: Report of the IMRT Subcommittee of the AAPM Radiation Therapy Committee." *Med Phys* 30:2089–2115. Also available as AAPM Report No. 82.
- Green, D., and P. C. Williams. *Linear Accelerators for Radiation Therapy*, 2nd Edition. Bristol, UK: IOP Publishing, 1997.
- Hall, E. J. *Radiobiology for the Radiologist, 5th Edition*. Philadelphia, PA: Lippincott Williams and Wilkins, 2000.
- Hendee, W. R., G. S. Ibbott, and E. G. Hendee. *Radiation Therapy Physics, 3rd Edition*. New York: John Wiley & Sons, Inc., 2004.
- Herman, M. G., J. M. Balter, D. A. Jaffray, K. P. McGee, P. Munro, S. Shalev, M. van Herk, and J. W. Wong. (2001). "Clinical use of electronic portal imaging: Report of AAPM Radiation Therapy Committee Task Group 58." *Med Phys* 29:712–737. Also available as AAPM Report No. 75.
- International Commission on Radiation Units and Measurements (ICRU). Report 62. Prescribing, Recording and Reporting Photon Beam Therapy (Supplement to ICRU Report 50). Bethesda, MD: ICRU, 1999.
- Johns, H. E., and J. R. Cunningham. *The Physics of Radiology, 4th Edition*. Springfield, IL: Charles C Thomas, 1983.
- Karzmark, C. J., and R. J. Morton. *A Primer on Theory and Operation of Linear Accelerators in Radiation Therapy, Second Edition*. Madison, WI: Medical Physics Publishing, 1998.
- Keall, P. (2004). "4-dimensional computed tomography imaging and treatment planning." *Semin Radiat Oncol* 14:81–90.

- Khan, F. M. *The Physics of Radiation Therapy, 2nd Edition*. Baltimore, MD: Lippincott Williams & Wilkins, 1994.
- Kutcher, G. J., L. Coia, M. Gillin, W. F. Hanson, S. Leibel, R. J. Morton, J. R. Palta, J. A. Purdy, L. E. Reinstein, G. K. Svensson, M. Weller, and L. Wingfield. (1994). "Comprehensive QA for radiation oncology: Report of AAPM Radiation Therapy Committee Task Group 40." *Med Phys* 21:581–618. Also available as AAPM Report No. 46.
- Langen, K. M., and D. T. L. Jones. (2001). "Organ motion and its management." *Int J Radiat Oncol Biol Phys* 50:265–278.
- Mackie, T. R., T. Holmes, and S. Swerdloff. (1993). "Tomotherapy: A new concept for the delivery of dynamic conformal radiotherapy." *Med Phys* 20:1709–1719.
- Mackie, T. R., J. Kapatoes, K. Ruchala, W. Lu, C. Wu, G. Olivera, L. Forrest, W. Tomé, J. Welsh, R. Jeraj, P. Harari, P. Reckwerdt, B. Paliwal, M. Ritter, H. Keller, J. Fowler, and M. Mehta. (2003). "Image guidance for precise conformal radiotherapy." *Int J Radiat Oncol Biol Phys* 56:89–105.
- Mageras, G. S., and E. Yorke. (2004). "Deep inspiration breath hold and respiratory gating strategies for reducing organ motion in radiation treatment." *Semin Radiat Oncol* 14:65–75.
- Murphy, M. J. (2004). "Tracking moving organs in real time." *Semin Radiat Oncol* 14:91–100.
- Papanikolaou, N., J. J. Battista, A. L. Boyer, C. Kappas, E. Klein, T. R. Mackie, M. Sharpe, and J. Van Dyk. AAPM Report No. 85. Tissue Inhomogeneity Corrections for Megavoltage Photon Beams: Report of Task Group No. 65 of the Radiation Therapy Committee of the American Association of Physicists in Medicine. Madison, WI: Medical Physics Publishing, 2004.
- Perez, C. A., and L. W. Brady. *Principles and Practice of Radiation Oncology*. Philadelphia, PA: J. B. Lippincott Company, 1987.
- Prado, K. L., and C. M. Prado. "Photon-Beam Dose Distributions and Treatment Planning" in *Principles and Practice of Radiation Therapy, 2nd Edition*. C. M. Washington and D. T. Leaver (Eds). St. Louis, MO: Mosby, Inc., 2004.
- Schell, M. C., F. J. Bova, D. A. Larson, D. D. Leavitt, W. R. Lutz, E. B. Podgorsak, and A. Wu. AAPM Report No. 54. Stereotactic Radiosurgery. Madison, WI: Medical Physics Publishing, 1995.
- Vargas, C., D. Yan, and L. L. Kestin. (2005). "Phase II dose escalation study of image-guided adaptive radiotherapy for prostate cancer: Use of dose-volume constraints to achieve rectal isototoxicity." *Int J Radiat Oncol Biol Phys* 63:141–149.
- Waldron, T. J. "Fundamental Requirements for IMRT" in *Intensity-Modulated Radiation Therapy: The State of the Art*. J. R. Palta and T. R. Mackie (Eds.). Madison, WI: Medical Physics Publishing, pp. 373–400, 2003.
- Wolbarst, A. B. *Physics of Radiology, 2nd Edition*. Madison, WI: Medical Physics Publishing, 2005.
- Wolbarst, A. B., L. Chin, and P. Stavros. "Radiotherapy Treatment Planning, Optimization of" in *Encyclopedia of Medical Devices and Instrumentation, Second Edition*. J. G. Webster (Ed.). Hoboken, NJ: John Wiley and Sons, 2006.
- Yan, D., F. Vicini, J. Wong, and A. Martinez. (1997). "Adaptive radiation therapy." *Phys Med Biol* 42:123–132.

